

Python results Hamaker coefficients for perpendicular [6,5], [9,0], [9,1], [9,3], and [29,0] cylinders in water using retarded and non-retarded formulations.

JC Hopkins

May 13, 2014

Abstract

Comparison of contributions of Matsubara sums to the retarded formulation for Hamaker coefficient, $\mathcal{A}^{(0)}$. I choose to use [6,5], a semiconductor, and [9,3], a semimetal, as examples. All calculations are for identical pairs of CNTs in water with a mutual angle of $\pi/2$.

Equations correspond to those in version 4 of Rudi's report.

Contents

1	CNTs	1
1.1	[6,5] Dielectric response spectrum, dispersion spectrum, and anisotropy measure	1
2	[9,0] dielectric response spectrum, dispersion spectrum, and anisotropy measure	2
3	[9,1] dielectric response spectrum, dispersion spectrum, and anisotropy measure	2
4	[9,3] dielectric response spectrum, dispersion spectrum, and anisotropy measure	3
5	[29,0] dielectric response spectrum, dispersion spectrum, and anisotropy measure	4
6	Semi-conductor [6,5]	5
6.1	[6,5] terms of Matsubara sum	5
6.2	[6,5] Log-log plot of $\mathcal{A}^{(0)}$ and $\mathcal{A}^{(2)}$	6
6.3	[6,5] Semi-log plot of $\mathcal{A}^{(0)}$ and $\mathcal{A}^{(2)}$	8

7	Semi-conductor [9,1]	8
7.1	[9,1] terms of Matsubara sum	8
7.2	[9,1] Log-log plot of $\mathcal{A}^{(0)}$ and $\mathcal{A}^{(2)}$	9
7.3	[9,1] Semi-log plot of $\mathcal{A}^{(0)}$ and $\mathcal{A}^{(2)}$	10
8	First results for semi-metal [9,3]	11
8.1	[9,3] terms of unmodified Matsubara sum	11
8.2	[9,3] terms of modified Matsubara sum with $\mathcal{A}(n=0)=0$	13
8.3	[9,3] Log-log plot of unmodified \mathcal{A}	14
8.4	[9,3] Log-log plot of modified $\mathcal{A}(n=0)=0$	15
8.5	[9,3] Semi-log plot of unmodified \mathcal{A}	16
8.6	[9,3] Semi-log plot of modified $\mathcal{A}(n=0)=0$	17
9	Semi-conductor [29,0]	18
9.1	[29,0] terms of Matsubara sum	18
9.2	[29,0] Log-log plot of $\mathcal{A}^{(0)}$ and $\mathcal{A}^{(2)}$	19
9.3	[29,0] Semi-log plot of $\mathcal{A}^{(0)}$ and $\mathcal{A}^{(2)}$	20
10	An example plot of knee: $\mathcal{A}^{(0)}$ for [9,3]	21
11	Plots of how each Matsubara term contributes to $\mathcal{A}_n^{(0)}(\ell)$	23
11.1	Plots for visualizing and comparing gradients for different CNT's	23
12	Fully Retarded	23
12.1	$\mathcal{A}^{(0)}$ for [6,5], [9,1], and [29,0] in water	23
12.2	Hamaker 2: $\mathcal{A}^{(2)}$ for [6,5], [9,1], and [29,0] in water	25
12.3	Total Hamaker: $\mathcal{A} = \mathcal{A}^{(0)} + \mathcal{A}^{(2)}$ for [6,5], [9,1], and [29,0] in water	27
13	Table of published results	28
14	Table of python results	28
15	Table of Gecko Hamaker results	29

1 CNTs

1.1 [6,5] Dielectric response spectrum, dispersion spectrum, and anisotropy measure

From the imaginary part of the dielectric response function of the carbon nanotubes,
we compute the London dispersion spectrum by the Kramers-Kronig transform:

$$\epsilon(i\zeta_n) = 1 + \frac{\pi}{2} \int_0^\infty dw \frac{\epsilon''(\omega)\omega}{\omega^2 + \zeta^2} \quad (1)$$

Relative anisotropy measures in the parallel and perpendicular direction are given by

$$\Delta_\perp = \frac{\epsilon_\perp^c - \epsilon_m}{\epsilon_\perp^c + \epsilon_m} \quad \Delta_\parallel = \frac{\epsilon_\parallel^c - \epsilon_m}{\epsilon_m}. \quad (2)$$

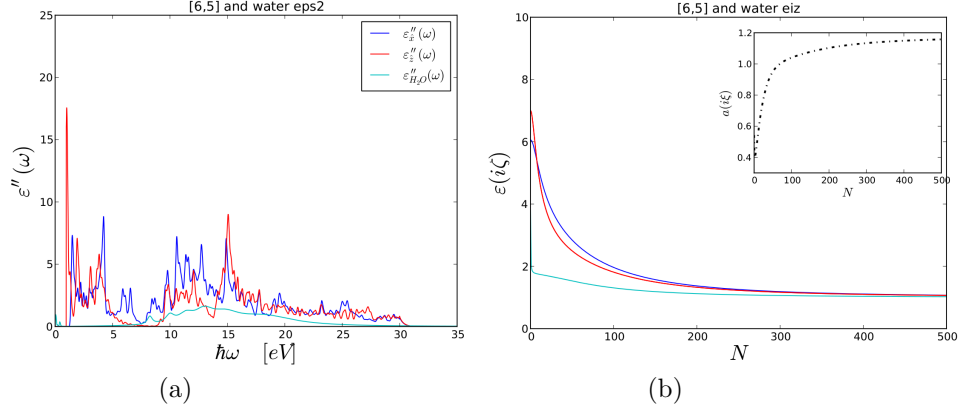


Figure 1: (a) Imaginary dielectric response spectrum, (b) dispersion spectrum and anisotropy measure (inset)

Ratio of anisotropy measure:

$$a_{1,2}(i\omega_n) = \frac{2\Delta_{\perp}^{(1,2)}(i\omega_n)}{\Delta_{\parallel}^{(1,2)}(i\omega_n)} = 2 \frac{(\epsilon_{\perp}^{c(1,2)}(i\omega_n) - \epsilon_m(i\omega_n))\epsilon_m(i\omega_n)}{(\epsilon_{\perp}^{c(1,2)}(i\omega_n) + \epsilon_m(i\omega_n))(\epsilon_{\parallel}^{c(1,2)}(i\omega_n) - \epsilon_m(i\omega_n))} \quad (3)$$

For interactions between identical CNTs, we set $a_1 = a_2$.

2 [9,0] dielectric response spectrum, dispersion spectrum, and anisotropy measure

Relative anisotropy measures in the parallel and perpendicular direction are given by

$$\Delta_{\perp} = \frac{\epsilon_{\perp}^c - \epsilon_m}{\epsilon_{\perp}^c + \epsilon_m} \quad \Delta_{\parallel} = \frac{\epsilon_{\parallel}^c - \epsilon_m}{\epsilon_m}. \quad (4)$$

Ratio of anisotropy measures

$$a_{1,2}(i\omega_n) = \frac{2\Delta_{\perp}^{(1,2)}(i\omega_n)}{\Delta_{\parallel}^{(1,2)}(i\omega_n)} = \frac{2(\epsilon_{\perp}^{c(1,2)}(i\omega_n) - \epsilon_m(i\omega_n))\epsilon_m(i\omega_n)}{(\epsilon_{\perp}^{c(1,2)}(i\omega_n) + \epsilon_m(i\omega_n))(\epsilon_{\parallel}^{c(1,2)}(i\omega_n) - \epsilon_m(i\omega_n))} \quad (5)$$

3 [9,1] dielectric response spectrum, dispersion spectrum, and anisotropy measure

Relative anisotropy measures in the parallel and perpendicular direction are given by

$$\Delta_{\perp} = \frac{\epsilon_{\perp}^c - \epsilon_m}{\epsilon_{\perp}^c + \epsilon_m} \quad \Delta_{\parallel} = \frac{\epsilon_{\parallel}^c - \epsilon_m}{\epsilon_m}. \quad (6)$$

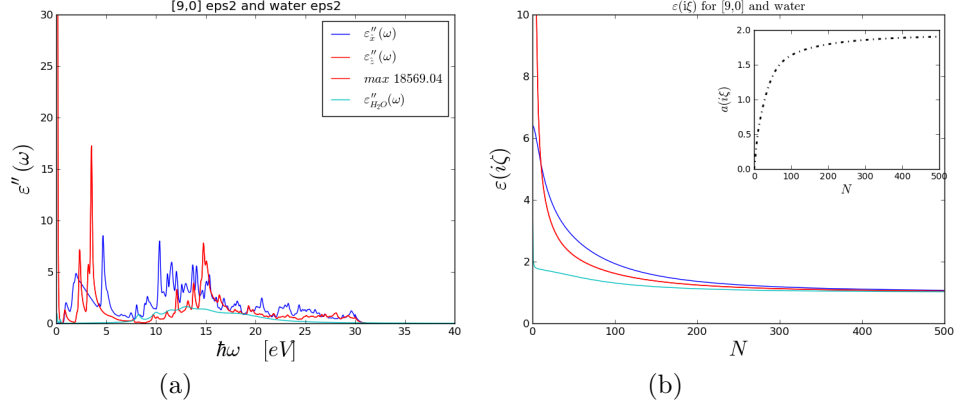


Figure 2: (a) Imaginary dielectric response spectrum, (b) dispersion spectrum and anisotropy measure (inset)

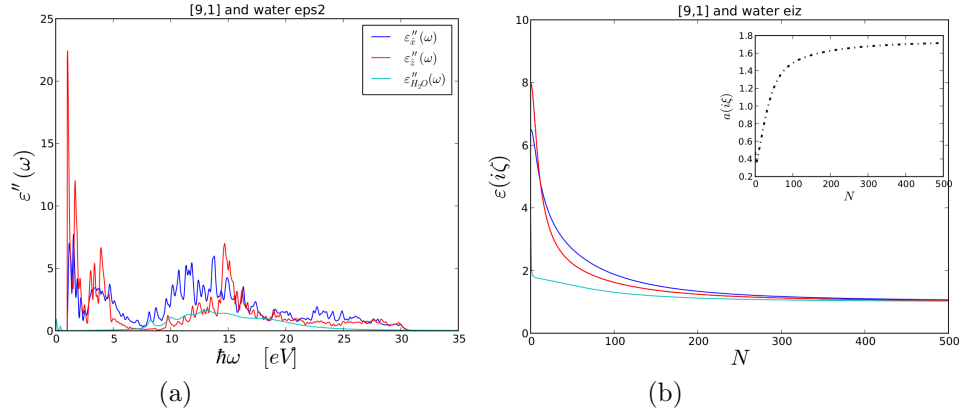


Figure 3: (a) Imaginary dielectric response spectrum, (b) dispersion spectrum and anisotropy measure (inset)

Ratio of anisotropy measures

$$a_{1,2}(i\omega_n) = \frac{2\Delta_{\perp}^{(1,2)}(i\omega_n)}{\Delta_{\parallel}^{(1,2)}(i\omega_n)} = 2 \frac{(\epsilon_{\perp}^{c(1,2)}(i\omega_n) - \epsilon_m(i\omega_n))\epsilon_m(i\omega_n)}{(\epsilon_{\perp}^{c(1,2)}(i\omega_n) + \epsilon_m(i\omega_n))(\epsilon_{\parallel}^{c(1,2)}(i\omega_n) - \epsilon_m(i\omega_n))} \quad (7)$$

4 [9,3] dielectric response spectrum, dispersion spectrum, and anisotropy measure

Relative anisotropy measures in the parallel and perpendicular direction are given by

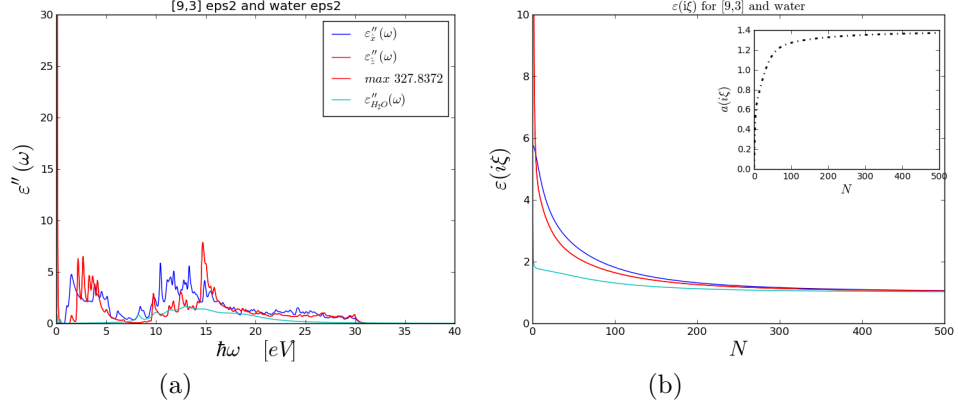


Figure 4: (a) Imaginary dielectric response spectrum, (b) dispersion spectrum and anisotropy measure (inset)

$$\Delta_{\perp} = \frac{\epsilon^c_{\perp} - \epsilon_m}{\epsilon^c_{\perp} + \epsilon_m} \quad \Delta_{\parallel} = \frac{\epsilon^c_{\parallel} - \epsilon_m}{\epsilon_m}. \quad (8)$$

Ratio of anisotropy measures

$$a_{1,2}(i\omega_n) = \frac{2\Delta_{\perp}^{(1,2)}(i\omega_n)}{\Delta_{\parallel}^{(1,2)}(i\omega_n)} = 2 \frac{(\epsilon^c_{\perp}{}^{(1,2)}(i\omega_n) - \epsilon_m(i\omega_n))\epsilon_m(i\omega_n)}{(\epsilon^c_{\perp}{}^{(1,2)}(i\omega_n) + \epsilon_m(i\omega_n))(\epsilon^c_{\parallel}{}^{(1,2)}(i\omega_n) - \epsilon_m(i\omega_n))} \quad (9)$$

5 [29,0] dielectric response spectrum, dispersion spectrum, and anisotropy measure

Relative anisotropy measures in the parallel and perpendicular direction are given by

$$\Delta_{\perp} = \frac{\epsilon^c_{\perp} - \epsilon_m}{\epsilon^c_{\perp} + \epsilon_m} \quad \Delta_{\parallel} = \frac{\epsilon^c_{\parallel} - \epsilon_m}{\epsilon_m}. \quad (10)$$

Ratio of anisotropy measures

$$a_{1,2}(i\omega_n) = \frac{2\Delta_{\perp}^{(1,2)}(i\omega_n)}{\Delta_{\parallel}^{(1,2)}(i\omega_n)} = 2 \frac{(\epsilon^c_{\perp}{}^{(1,2)}(i\omega_n) - \epsilon_m(i\omega_n))\epsilon_m(i\omega_n)}{(\epsilon^c_{\perp}{}^{(1,2)}(i\omega_n) + \epsilon_m(i\omega_n))(\epsilon^c_{\parallel}{}^{(1,2)}(i\omega_n) - \epsilon_m(i\omega_n))} \quad (11)$$

Fully retarded Hamaker Coefficients for Matsubara Sum

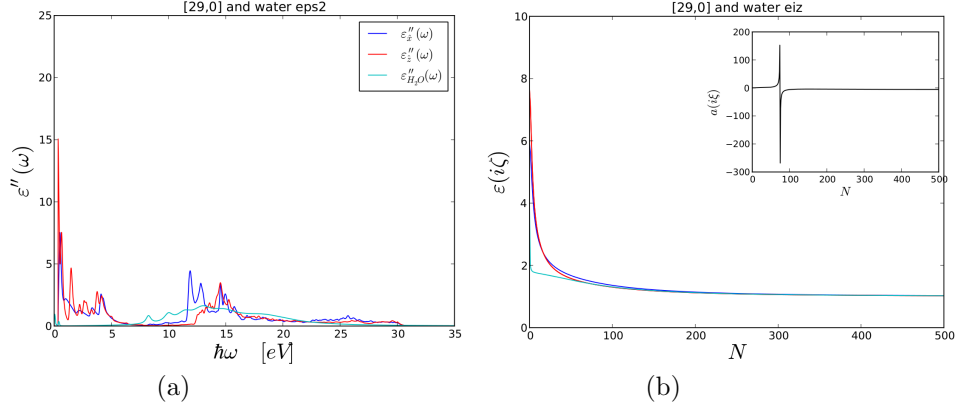


Figure 5: (a) Imaginary dielectric response spectrum, (b) dispersion spectrum and anisotropy measure (inset)

6 Semi-conductor [6,5]

6.1 [6,5] terms of Matsubara sum

We write the Hamaker coefficients as,

$$\mathcal{A}^{(0)}(\ell) = \frac{k_B T}{32} \sum_{n=0}^{\infty} \Delta_{1,\parallel} \Delta_{2,\parallel} p_n^4(\ell) \int_0^\infty t dt \frac{e^{-2p_n(\ell)\sqrt{t^2+1}}}{(t^2+1)} \tilde{g}^{(0)}(t, a_1(i\omega_n), a_2(i\omega_n)) \quad (12)$$

with

$$\tilde{g}^{(0)}(t, a_1(i\omega_n), a_2(i\omega_n)) = 2 \left[(1+3a_1)(1+3a_2)t^4 + 2(1+2a_1+2a_2+3a_1a_2)t^2 + 2(1+a_1)(1+a_2) \right]$$

and

$$\mathcal{A}^{(2)}(\ell) = \frac{k_B T}{32} \sum_{n=0}^{\infty} \Delta_{1,\parallel} \Delta_{2,\parallel} p_n^4(\ell) \int_0^\infty t dt \frac{e^{-2p_n(\ell)\sqrt{t^2+1}}}{(t^2+1)} \tilde{g}^{(2)}(t, a_1(i\omega_n), a_2(i\omega_n), \theta) \quad (13)$$

with

$$\tilde{g}^{(2)}(t, a_1(i\omega_n), a_2(i\omega_n), \theta) = (1-a_1)(1-a_2)(t^2+2)^2$$

Where

$$p_n^2(\ell) = \epsilon_m(i\omega_n) \frac{\omega_n^2}{c^2} \ell^2,$$

$$\Delta_\perp = \frac{\epsilon_\perp^c - \epsilon_m}{\epsilon_\perp^c + \epsilon_m} \quad \Delta_\parallel = \frac{\epsilon_\parallel^c - \epsilon_m}{\epsilon_m},$$

$$a = \frac{2\Delta_\perp}{\Delta_\parallel} = 2 \frac{(\epsilon_\perp^c - \epsilon_m)\epsilon_m}{(\epsilon_\perp^c + \epsilon_m)(\epsilon_\parallel^c - \epsilon_m)}$$

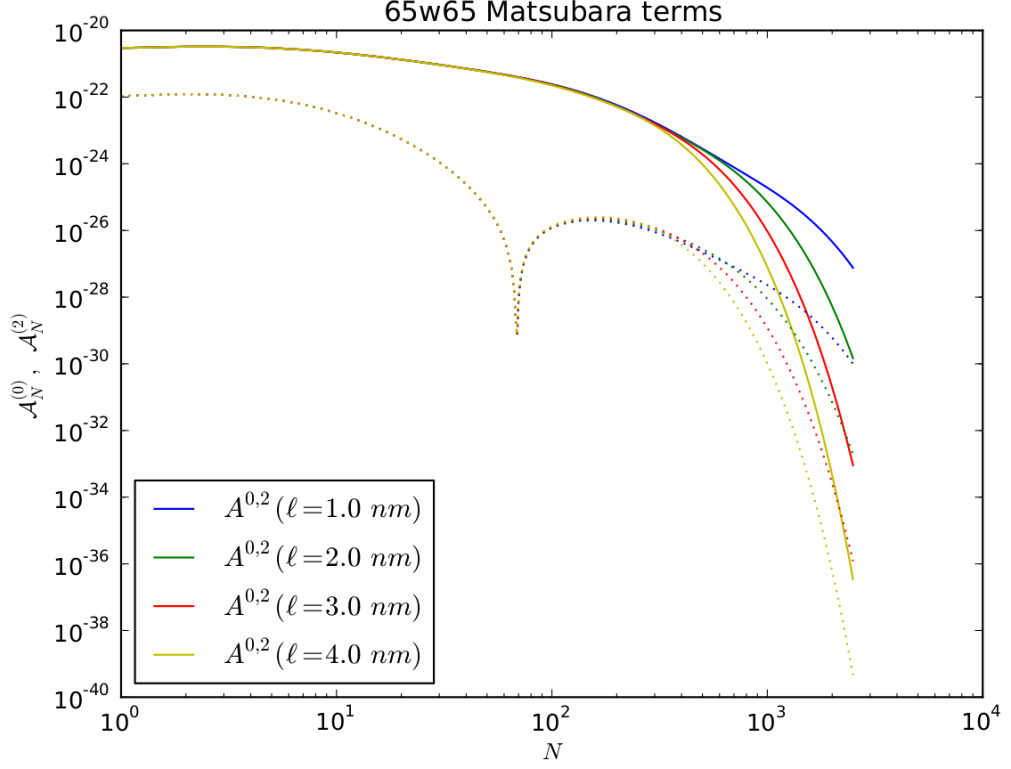


Figure 6: Terms contributing to Matsubara sum as a function of N

For $n = 0$, we use

$$\mathcal{A}_{n=0}^{(0)}(\ell) = \frac{1}{2} \frac{k_B T}{32} \Delta_{1,\parallel} \Delta_{2,\parallel} \int_0^\infty u^3 du e^{-2u} [2(1+3a_1)(1+3a_2)] \quad (14)$$

and

$$\mathcal{A}_{n=0}^{(2)}(\ell) = \frac{1}{2} \frac{k_B T}{32} \Delta_{1,\parallel} \Delta_{2,\parallel} \int_0^\infty u^3 du e^{-2u} [(1-a_1)(1-a_2)] \quad (15)$$

where $u = Ql$.

6.2 [6,5] Log-log plot of $\mathcal{A}^{(0)}$ and $\mathcal{A}^{(2)}$

$$\mathcal{A}^{(0)}(\ell) = \frac{k_B T}{32} \sum_{n=0}^{\infty} \Delta_{1,\parallel} \Delta_{2,\parallel} p_n^4(\ell) \int_0^\infty t dt \frac{e^{-2p_n(\ell)\sqrt{t^2+1}}}{(t^2+1)} \tilde{g}^{(0)}(t, a_1(i\omega_n), a_2(i\omega_n)) \quad (16)$$

with

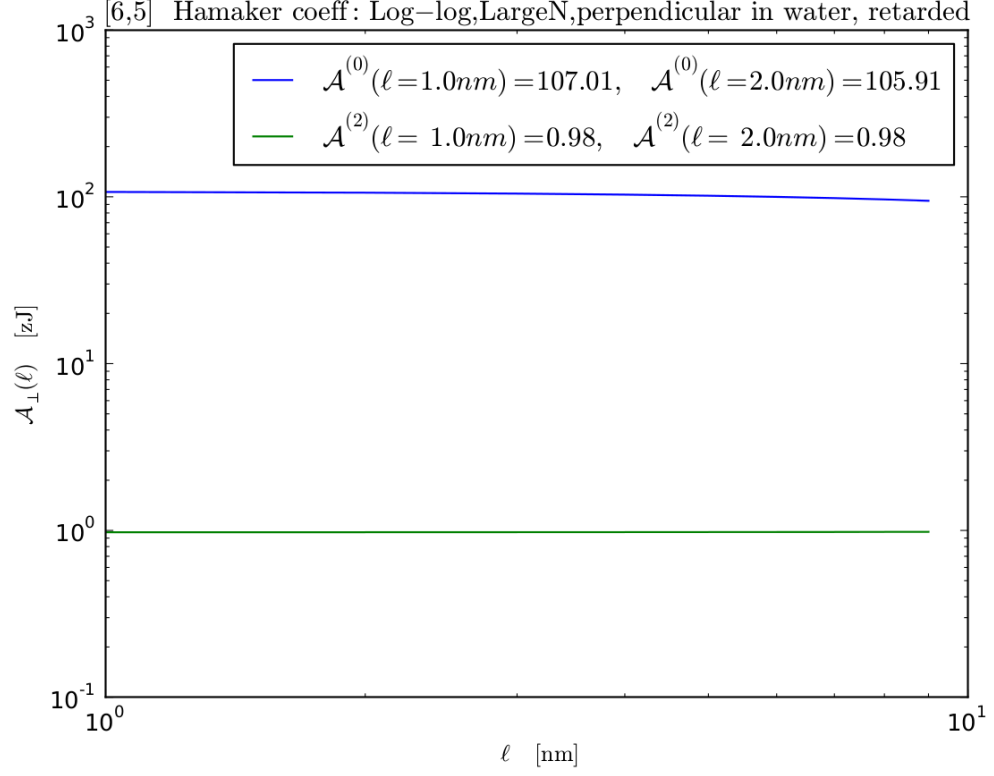


Figure 7: Full result

$$\tilde{g}^{(0)}(t, a_1(i\omega_n), a_2(i\omega_n)) = 2 \left[(1 + 3a_1)(1 + 3a_2)t^4 + 2(1 + 2a_1 + 2a_2 + 3a_1a_2)t^2 + 2(1 + a_1)(1 + a_2) \right]$$

and

$$\mathcal{A}^{(2)}(\ell) = \frac{k_B T}{32} \sum_{n=0}^{\infty} \Delta_{1,\parallel} \Delta_{2,\parallel} p_n^4(\ell) \int_0^\infty t dt \frac{e^{-2p_n(\ell)\sqrt{t^2+1}}}{(t^2+1)} \tilde{g}^{(2)}(t, a_1(i\omega_n), a_2(i\omega_n), \theta) \quad (17)$$

with

$$\tilde{g}^{(2)}(t, a_1(i\omega_n), a_2(i\omega_n), \theta) = (1 - a_1)(1 - a_2)(t^2 + 2)^2 \quad (18)$$

6.3 [6,5] Semi-log plot of $\mathcal{A}^{(0)}$ and $\mathcal{A}^{(2)}$

$$\mathcal{A}^{(0)}(\ell) = \frac{k_B T}{32} \sum_{n=0}^{\infty'} \Delta_{1,\parallel} \Delta_{2,\parallel} p_n^4(\ell) \int_0^\infty t dt \frac{e^{-2p_n(\ell)\sqrt{t^2+1}}}{(t^2+1)} \tilde{g}^{(0)}(t, a_1(i\omega_n), a_2(i\omega_n)) \quad (19)$$

with

$$\tilde{g}^{(0)}(t, a_1(i\omega_n), a_2(i\omega_n)) = 2 \left[(1+3a_1)(1+3a_2)t^4 + 2(1+2a_1+2a_2+3a_1a_2)t^2 + 2(1+a_1)(1+a_2) \right]$$

and

$$\mathcal{A}^{(2)}(\ell) = \frac{k_B T}{32} \sum_{n=0}^{\infty'} \Delta_{1,\parallel} \Delta_{2,\parallel} p_n^4(\ell) \int_0^\infty t dt \frac{e^{-2p_n(\ell)\sqrt{t^2+1}}}{(t^2+1)} \tilde{g}^{(2)}(t, a_1(i\omega_n), a_2(i\omega_n), \theta) \quad (20)$$

with

$$\tilde{g}^{(2)}(t, a_1(i\omega_n), a_2(i\omega_n), \theta) = (1-a_1)(1-a_2)(t^2+2)^2 \quad (21)$$

7 Semi-conductor [9,1]

7.1 [9,1] terms of Matsubara sum

$$\mathcal{A}^{(0)}(\ell) = \frac{k_B T}{32} \sum_{n=0}^{\infty'} \Delta_{1,\parallel} \Delta_{2,\parallel} p_n^4(\ell) \int_0^\infty t dt \frac{e^{-2p_n(\ell)\sqrt{t^2+1}}}{(t^2+1)} \tilde{g}^{(0)}(t, a_1(i\omega_n), a_2(i\omega_n)) \quad (22)$$

with

$$\tilde{g}^{(0)}(t, a_1(i\omega_n), a_2(i\omega_n)) = 2 \left[(1+3a_1)(1+3a_2)t^4 + 2(1+2a_1+2a_2+3a_1a_2)t^2 + 2(1+a_1)(1+a_2) \right]$$

and

$$\mathcal{A}^{(2)}(\ell) = \frac{k_B T}{32} \sum_{n=0}^{\infty'} \Delta_{1,\parallel} \Delta_{2,\parallel} p_n^4(\ell) \int_0^\infty t dt \frac{e^{-2p_n(\ell)\sqrt{t^2+1}}}{(t^2+1)} \tilde{g}^{(2)}(t, a_1(i\omega_n), a_2(i\omega_n), \theta) \quad (23)$$

with

$$\tilde{g}^{(2)}(t, a_1(i\omega_n), a_2(i\omega_n), \theta) = (1-a_1)(1-a_2)(t^2+2)^2 \quad (24)$$

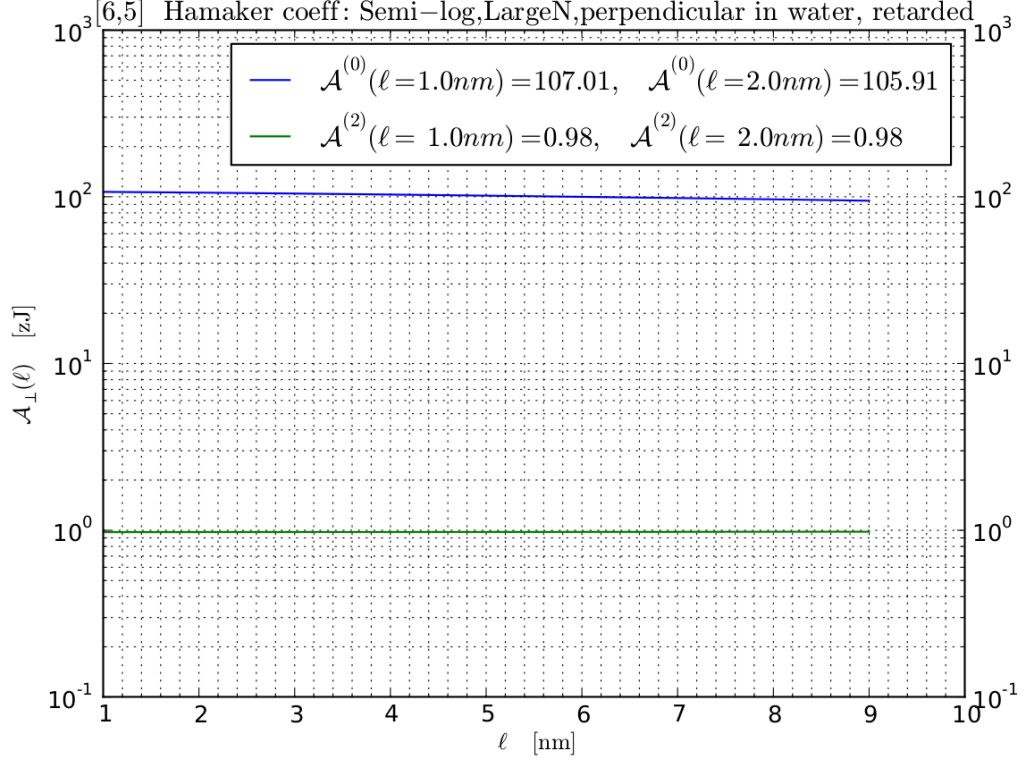


Figure 8: Full result

7.2 [9,1] Log-log plot of $\mathcal{A}^{(0)}$ and $\mathcal{A}^{(2)}$

$$\mathcal{A}^{(0)}(\ell) = \frac{k_B T}{32} \sum_{n=0}^{\infty} \Delta_{1,\parallel} \Delta_{2,\parallel} p_n^4(\ell) \int_0^\infty t dt \frac{e^{-2p_n(\ell)\sqrt{t^2+1}}}{(t^2+1)} \tilde{g}^{(0)}(t, a_1(i\omega_n), a_2(i\omega_n)) \quad (25)$$

with

$$\tilde{g}^{(0)}(t, a_1(i\omega_n), a_2(i\omega_n)) = 2 \left[(1+3a_1)(1+3a_2)t^4 + 2(1+2a_1+2a_2+3a_1a_2)t^2 + 2(1+a_1)(1+a_2) \right]$$

and

$$\mathcal{A}^{(2)}(\ell) = \frac{k_B T}{32} \sum_{n=0}^{\infty} \Delta_{1,\parallel} \Delta_{2,\parallel} p_n^4(\ell) \int_0^\infty t dt \frac{e^{-2p_n(\ell)\sqrt{t^2+1}}}{(t^2+1)} \tilde{g}^{(2)}(t, a_1(i\omega_n), a_2(i\omega_n), \theta) \quad (26)$$

with

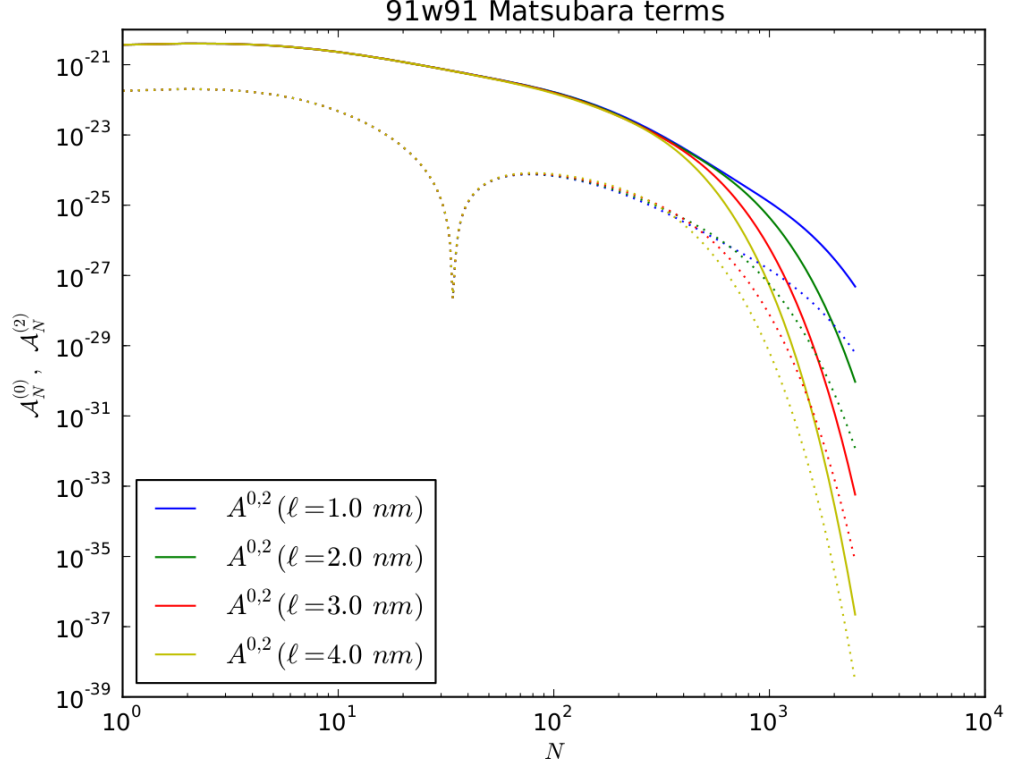


Figure 9: Terms contributing to Matsubara sum as a function of N

$$\tilde{g}^{(2)}(t, a_1(i\omega_n), a_2(i\omega_n), \theta) = (1 - a_1)(1 - a_2)(t^2 + 2)^2 \quad (27)$$

7.3 [9,1] Semi-log plot of $\mathcal{A}^{(0)}$ and $\mathcal{A}^{(2)}$

$$\mathcal{A}^{(0)}(\ell) = \frac{k_B T}{32} \sum_{n=0}^{\infty} \Delta_{1,\parallel} \Delta_{2,\parallel} p_n^4(\ell) \int_0^\infty t dt \frac{e^{-2p_n(\ell)\sqrt{t^2+1}}}{(t^2+1)} \tilde{g}^{(0)}(t, a_1(i\omega_n), a_2(i\omega_n)) \quad (28)$$

with

$$\tilde{g}^{(0)}(t, a_1(i\omega_n), a_2(i\omega_n)) = 2 \left[(1 + 3a_1)(1 + 3a_2)t^4 + 2(1 + 2a_1 + 2a_2 + 3a_1a_2)t^2 + 2(1 + a_1)(1 + a_2) \right]$$

and

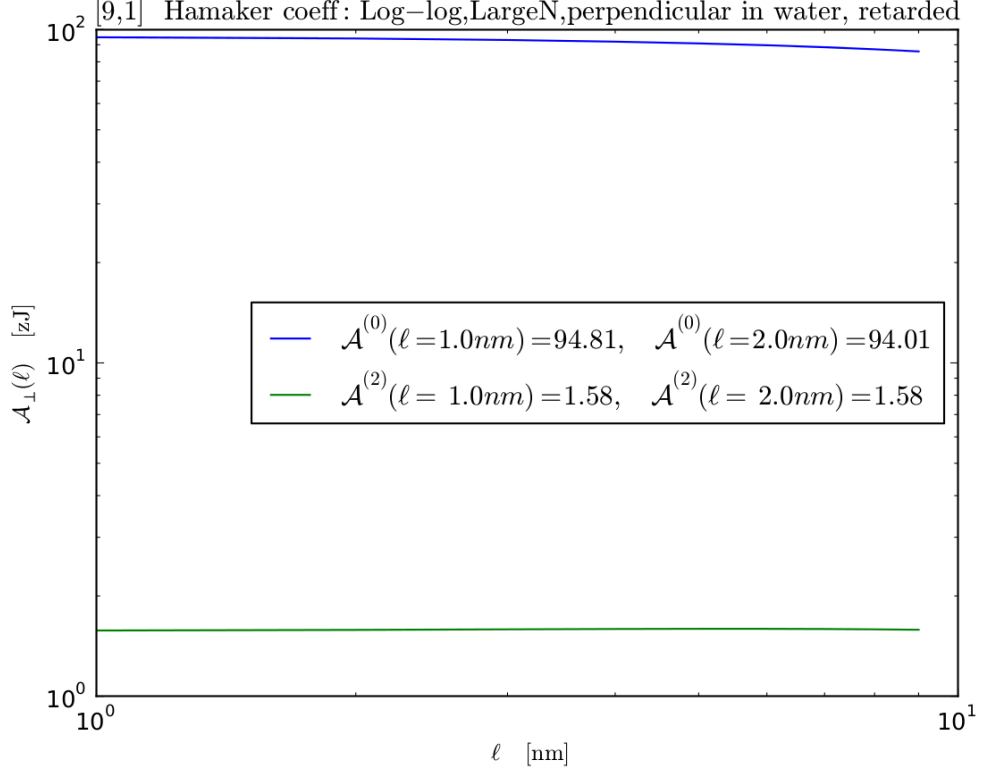


Figure 10: Full result

$$\mathcal{A}^{(2)}(\ell) = \frac{k_B T}{32} \sum_{n=0}^{\infty} \Delta_{1,\parallel} \Delta_{2,\parallel} p_n^4(\ell) \int_0^\infty t dt \frac{e^{-2p_n(\ell)\sqrt{t^2+1}}}{(t^2+1)} \tilde{g}^{(2)}(t, a_1(i\omega_n), a_2(i\omega_n), \theta) \quad (29)$$

with

$$\tilde{g}^{(2)}(t, a_1(i\omega_n), a_2(i\omega_n), \theta) = (1 - a_1)(1 - a_2)(t^2 + 2)^2 \quad (30)$$

8 First results for semi-metal [9,3]

8.1 [9,3] terms of unmodified Matsubara sum

$$\mathcal{A}^{(0)}(\ell) = \frac{k_B T}{32} \sum_{n=0}^{\infty} \Delta_{1,\parallel} \Delta_{2,\parallel} p_n^4(\ell) \int_0^\infty t dt \frac{e^{-2p_n(\ell)\sqrt{t^2+1}}}{(t^2+1)} \tilde{g}^{(0)}(t, a_1(i\omega_n), a_2(i\omega_n)) \quad (31)$$

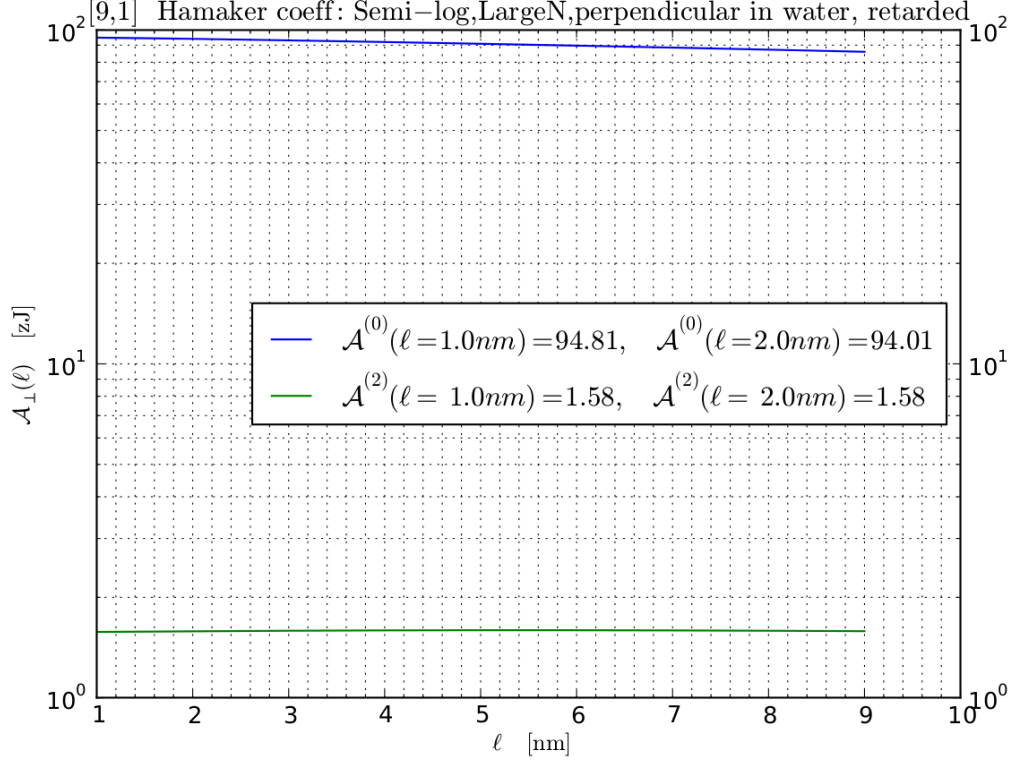


Figure 11: Full result

with

$$\tilde{g}^{(0)}(t, a_1(i\omega_n), a_2(i\omega_n)) = 2 \left[(1 + 3a_1)(1 + 3a_2)t^4 + 2(1 + 2a_1 + 2a_2 + 3a_1a_2)t^2 + 2(1 + a_1)(1 + a_2) \right]$$

and

$$\mathcal{A}^{(2)}(\ell) = \frac{k_B T}{32} \sum_{n=0}^{\infty} \Delta_{1,\parallel} \Delta_{2,\parallel} p_n^4(\ell) \int_0^{\infty} t dt \frac{e^{-2p_n(\ell)\sqrt{t^2+1}}}{(t^2+1)} \tilde{g}^{(2)}(t, a_1(i\omega_n), a_2(i\omega_n), \theta) \quad (32)$$

with

$$\tilde{g}^{(2)}(t, a_1(i\omega_n), a_2(i\omega_n), \theta) = (1 - a_1)(1 - a_2)(t^2 + 2)^2 \quad (33)$$

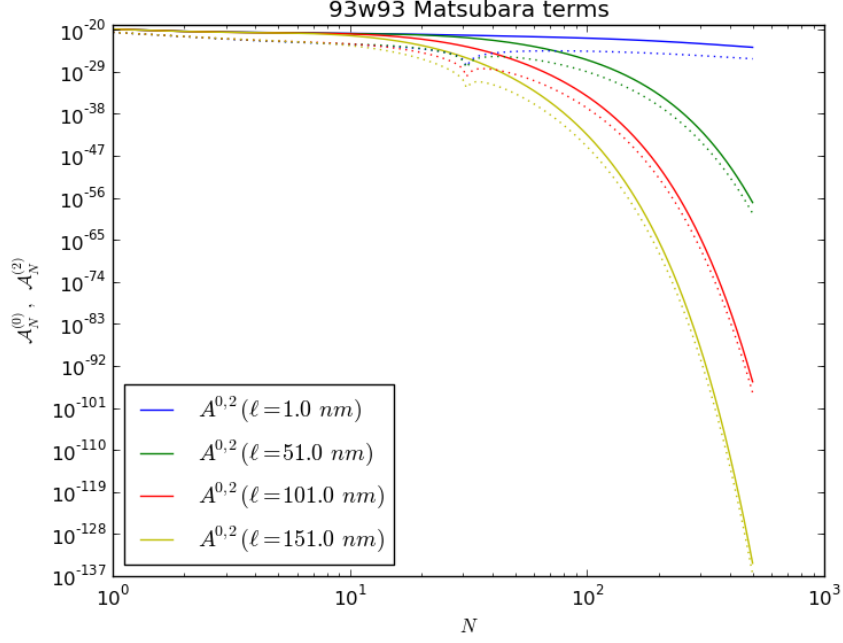


Figure 12: Full result

8.2 [9,3] terms of modified Matsubara sum with

$$\mathcal{A}(n=0) = 0$$

$$\mathcal{A}^{(0)}(\ell) = \frac{k_B T}{32} \sum_{n=0}^{\infty} \Delta_{1,\parallel} \Delta_{2,\parallel} p_n^4(\ell) \int_0^{\infty} t dt \frac{e^{-2p_n(\ell)\sqrt{t^2+1}}}{(t^2+1)} \tilde{g}^{(0)}(t, a_1(i\omega_n), a_2(i\omega_n)) \quad (34)$$

with

$$\tilde{g}^{(0)}(t, a_1(i\omega_n), a_2(i\omega_n)) = 2 [(1+3a_1)(1+3a_2)t^4 + 2(1+2a_1+2a_2+3a_1a_2)t^2 + 2(1+a_1)(1+a_2)] \quad (35)$$

and

$$\mathcal{A}^{(2)}(\ell) = \frac{k_B T}{32} \sum_{n=0}^{\infty} \Delta_{1,\parallel} \Delta_{2,\parallel} p_n^4(\ell) \int_0^{\infty} t dt \frac{e^{-2p_n(\ell)\sqrt{t^2+1}}}{(t^2+1)} \tilde{g}^{(2)}(t, a_1(i\omega_n), a_2(i\omega_n), \theta) \quad (36)$$

with

$$\tilde{g}^{(2)}(t, a_1(i\omega_n), a_2(i\omega_n), \theta) = (1-a_1)(1-a_2)(t^2+2)^2 \quad (37)$$

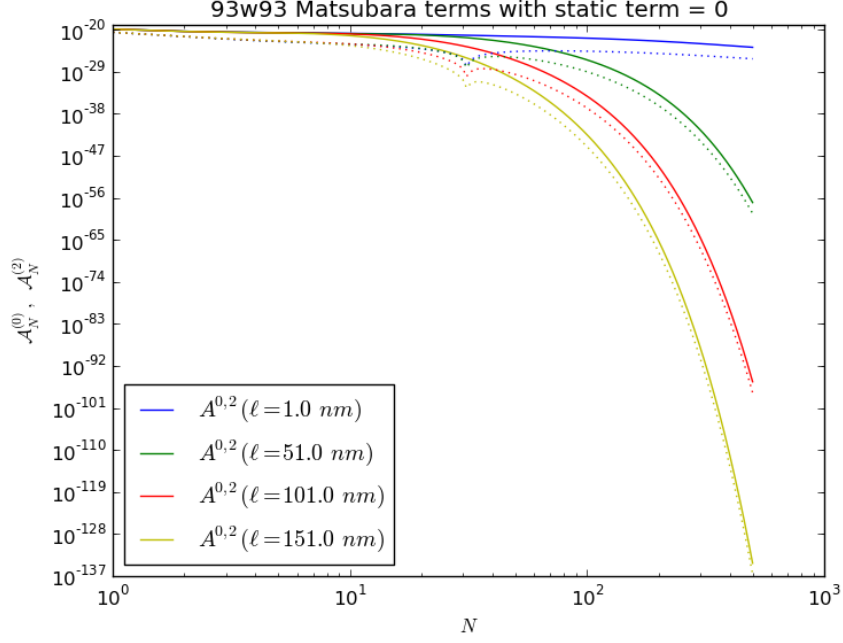


Figure 13: Full result

8.3 [9,3] Log-log plot of unmodified \mathcal{A}

$$\mathcal{A}^{(0)}(\ell) = \frac{k_B T}{32} \sum_{n=0}^{\infty} \Delta_{1,\parallel} \Delta_{2,\parallel} p_n^4(\ell) \int_0^{\infty} t dt \frac{e^{-2p_n(\ell)\sqrt{t^2+1}}}{(t^2+1)} \tilde{g}^{(0)}(t, a_1(i\omega_n), a_2(i\omega_n)) \quad (38)$$

with

$$\tilde{g}^{(0)}(t, a_1(i\omega_n), a_2(i\omega_n)) = 2 \left[(1 + 3a_1)(1 + 3a_2)t^4 + 2(1 + 2a_1 + 2a_2 + 3a_1a_2)t^2 + 2(1 + a_1)(1 + a_2) \right]$$

and

$$\mathcal{A}^{(2)}(\ell) = \frac{k_B T}{32} \sum_{n=0}^{\infty} \Delta_{1,\parallel} \Delta_{2,\parallel} p_n^4(\ell) \int_0^{\infty} t dt \frac{e^{-2p_n(\ell)\sqrt{t^2+1}}}{(t^2+1)} \tilde{g}^{(2)}(t, a_1(i\omega_n), a_2(i\omega_n), \theta) \quad (39)$$

with

$$\tilde{g}^{(2)}(t, a_1(i\omega_n), a_2(i\omega_n), \theta) = (1 - a_1)(1 - a_2)(t^2 + 2)^2 \quad (40)$$

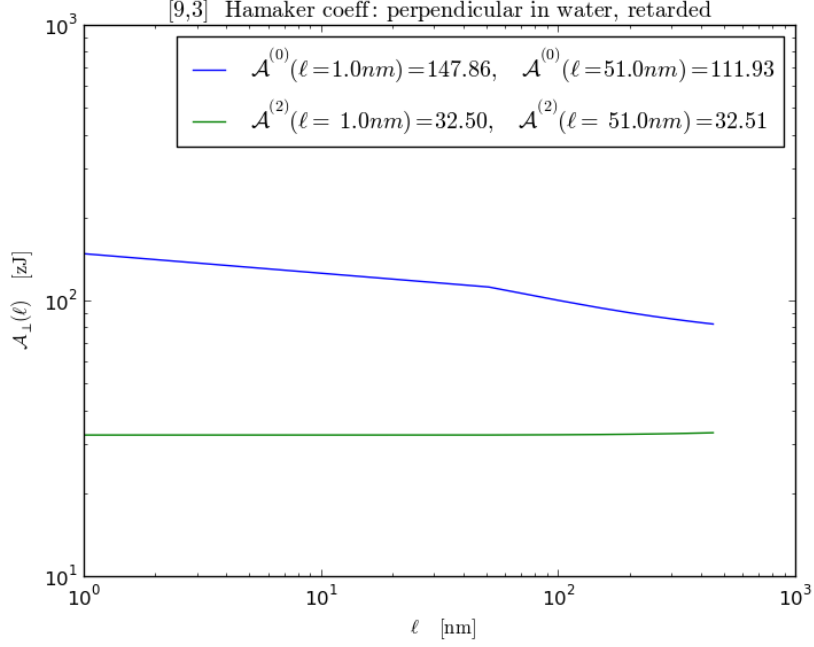


Figure 14: Full result

8.4 [9,3] Log-log plot of modified $\mathcal{A}(n=0) = 0$

$$\mathcal{A}^{(0)}(\ell) = \frac{k_B T}{32} \sum_{n=0}^{\infty} \Delta_{1,\parallel} \Delta_{2,\parallel} p_n^4(\ell) \int_0^\infty t dt \frac{e^{-2p_n(\ell)\sqrt{t^2+1}}}{(t^2+1)} \tilde{g}^{(0)}(t, a_1(i\omega_n), a_2(i\omega_n)) \quad (41)$$

with

$$\tilde{g}^{(0)}(t, a_1(i\omega_n), a_2(i\omega_n)) = 2 \left[(1 + 3a_1)(1 + 3a_2)t^4 + 2(1 + 2a_1 + 2a_2 + 3a_1a_2)t^2 + 2(1 + a_1)(1 + a_2) \right]$$

and

$$\mathcal{A}^{(2)}(\ell) = \frac{k_B T}{32} \sum_{n=0}^{\infty} \Delta_{1,\parallel} \Delta_{2,\parallel} p_n^4(\ell) \int_0^\infty t dt \frac{e^{-2p_n(\ell)\sqrt{t^2+1}}}{(t^2+1)} \tilde{g}^{(2)}(t, a_1(i\omega_n), a_2(i\omega_n), \theta) \quad (42)$$

with

$$\tilde{g}^{(2)}(t, a_1(i\omega_n), a_2(i\omega_n), \theta) = (1 - a_1)(1 - a_2)(t^2 + 2)^2 \quad (43)$$

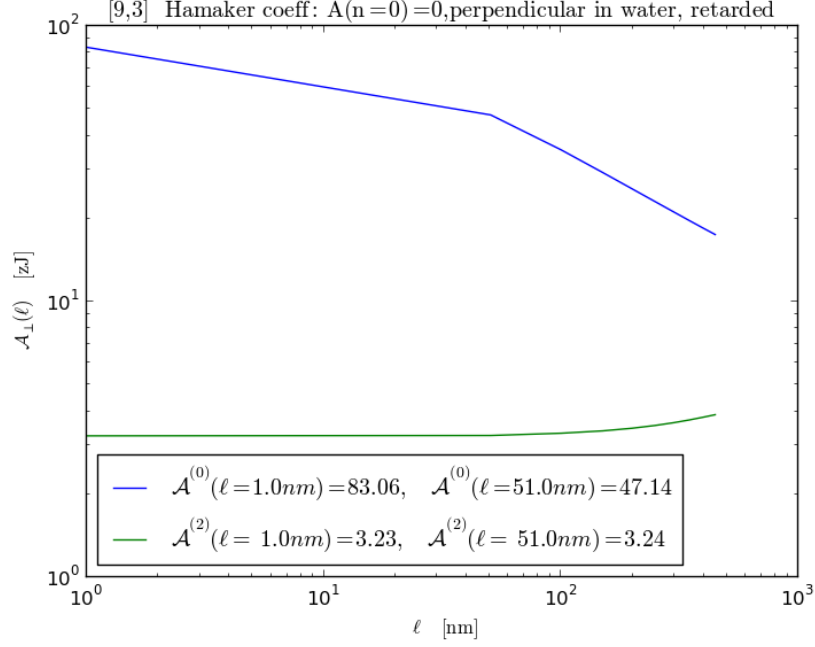


Figure 15: Full result

8.5 [9,3] Semi-log plot of unmodified \mathcal{A}

$$\mathcal{A}^{(0)}(\ell) = \frac{k_B T}{32} \sum_{n=0}^{\infty} \Delta_{1,\parallel} \Delta_{2,\parallel} p_n^4(\ell) \int_0^\infty t dt \frac{e^{-2p_n(\ell)\sqrt{t^2+1}}}{(t^2+1)} \tilde{g}^{(0)}(t, a_1(i\omega_n), a_2(i\omega_n)) \quad (44)$$

with

$$\tilde{g}^{(0)}(t, a_1(i\omega_n), a_2(i\omega_n)) = 2 \left[(1 + 3a_1)(1 + 3a_2)t^4 + 2(1 + 2a_1 + 2a_2 + 3a_1a_2)t^2 + 2(1 + a_1)(1 + a_2) \right]$$

and

$$\mathcal{A}^{(2)}(\ell) = \frac{k_B T}{32} \sum_{n=0}^{\infty} \Delta_{1,\parallel} \Delta_{2,\parallel} p_n^4(\ell) \int_0^\infty t dt \frac{e^{-2p_n(\ell)\sqrt{t^2+1}}}{(t^2+1)} \tilde{g}^{(2)}(t, a_1(i\omega_n), a_2(i\omega_n), \theta) \quad (45)$$

with

$$\tilde{g}^{(2)}(t, a_1(i\omega_n), a_2(i\omega_n), \theta) = (1 - a_1)(1 - a_2)(t^2 + 2)^2 \quad (46)$$

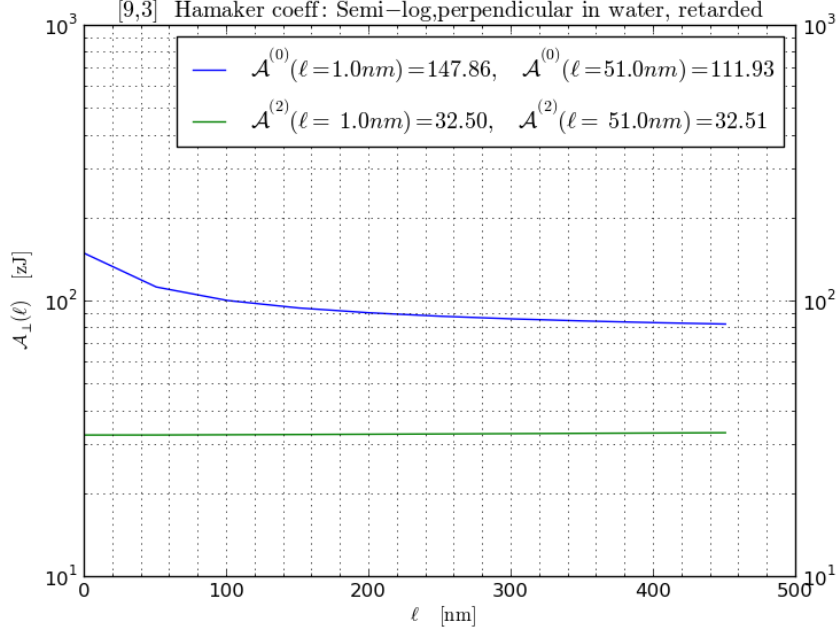


Figure 16: Full result

8.6 [9,3] Semi-log plot of modified $\mathcal{A}(n=0) = 0$

$$\mathcal{A}^{(0)}(\ell) = \frac{k_B T}{32} \sum_{n=0}^{\infty} \Delta_{1,\parallel} \Delta_{2,\parallel} p_n^4(\ell) \int_0^\infty t dt \frac{e^{-2p_n(\ell)\sqrt{t^2+1}}}{(t^2+1)} \tilde{g}^{(0)}(t, a_1(i\omega_n), a_2(i\omega_n)) \quad (47)$$

with

$$\tilde{g}^{(0)}(t, a_1(i\omega_n), a_2(i\omega_n)) = 2 \left[(1 + 3a_1)(1 + 3a_2)t^4 + 2(1 + 2a_1 + 2a_2 + 3a_1a_2)t^2 + 2(1 + a_1)(1 + a_2) \right]$$

and

$$\mathcal{A}^{(2)}(\ell) = \frac{k_B T}{32} \sum_{n=0}^{\infty} \Delta_{1,\parallel} \Delta_{2,\parallel} p_n^4(\ell) \int_0^\infty t dt \frac{e^{-2p_n(\ell)\sqrt{t^2+1}}}{(t^2+1)} \tilde{g}^{(2)}(t, a_1(i\omega_n), a_2(i\omega_n), \theta) \quad (48)$$

with

$$\tilde{g}^{(2)}(t, a_1(i\omega_n), a_2(i\omega_n), \theta) = (1 - a_1)(1 - a_2)(t^2 + 2)^2 \quad (49)$$

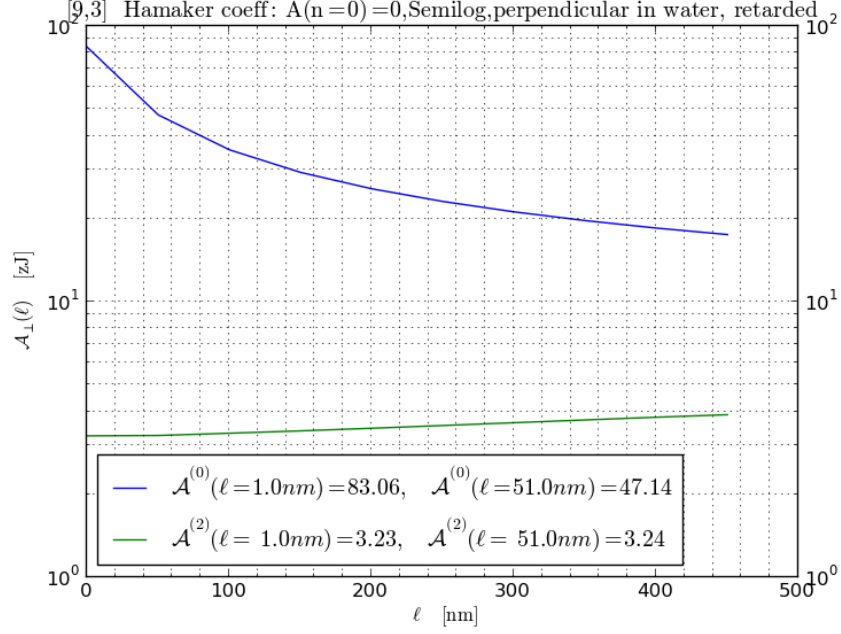


Figure 17: Full result

9 Semi-conductor [29,0]

9.1 [29,0] terms of Matsubara sum

$$\mathcal{A}^{(0)}(\ell) = \frac{k_B T}{32} \sum_{n=0}^{\infty} \Delta_{1,\parallel} \Delta_{2,\parallel} p_n^4(\ell) \int_0^{\infty} t dt \frac{e^{-2p_n(\ell)\sqrt{t^2+1}}}{(t^2+1)} \tilde{g}^{(0)}(t, a_1(i\omega_n), a_2(i\omega_n)) \quad (50)$$

with

$$\tilde{g}^{(0)}(t, a_1(i\omega_n), a_2(i\omega_n)) = 2 \left[(1 + 3a_1)(1 + 3a_2)t^4 + 2(1 + 2a_1 + 2a_2 + 3a_1a_2)t^2 + 2(1 + a_1)(1 + a_2) \right]$$

and

$$\mathcal{A}^{(2)}(\ell) = \frac{k_B T}{32} \sum_{n=0}^{\infty} \Delta_{1,\parallel} \Delta_{2,\parallel} p_n^4(\ell) \int_0^{\infty} t dt \frac{e^{-2p_n(\ell)\sqrt{t^2+1}}}{(t^2+1)} \tilde{g}^{(2)}(t, a_1(i\omega_n), a_2(i\omega_n), \theta) \quad (51)$$

with

$$\tilde{g}^{(2)}(t, a_1(i\omega_n), a_2(i\omega_n), \theta) = (1 - a_1)(1 - a_2)(t^2 + 2)^2 \quad (52)$$

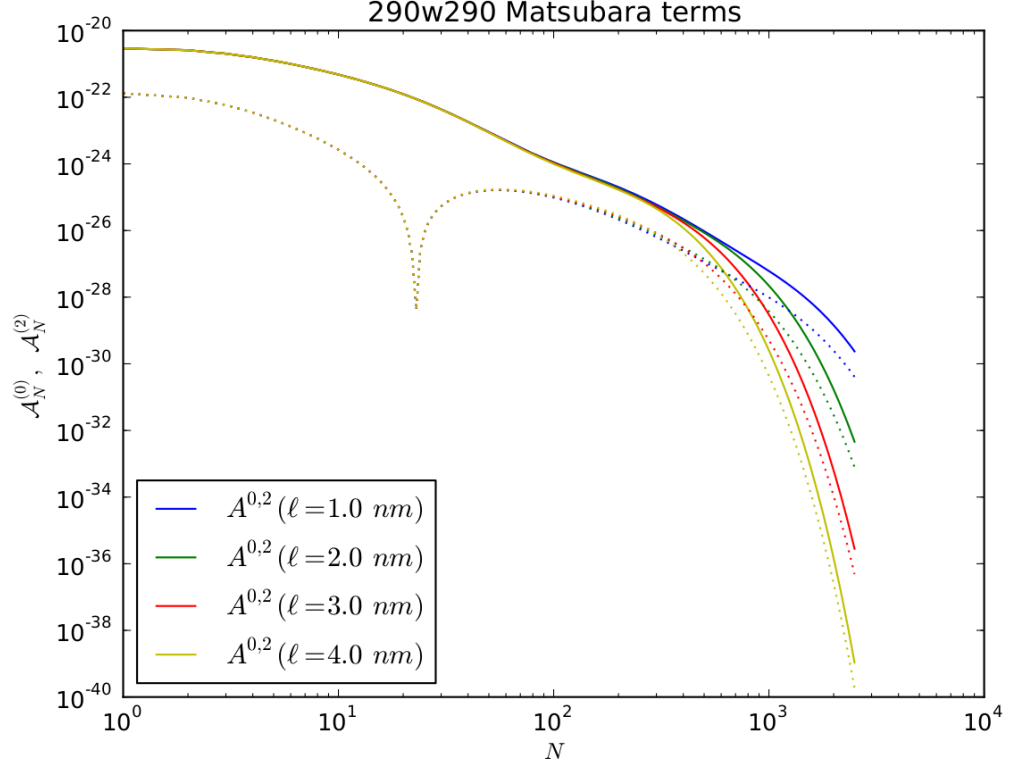


Figure 18: Full result

9.2 [29,0] Log-log plot of $\mathcal{A}^{(0)}$ and $\mathcal{A}^{(2)}$

$$\mathcal{A}^{(0)}(\ell) = \frac{k_B T}{32} \sum_{n=0}^{\infty} \Delta_{1,\parallel} \Delta_{2,\parallel} p_n^4(\ell) \int_0^\infty t dt \frac{e^{-2p_n(\ell)\sqrt{t^2+1}}}{(t^2+1)} \tilde{g}^{(0)}(t, a_1(i\omega_n), a_2(i\omega_n)) \quad (53)$$

with

$$\tilde{g}^{(0)}(t, a_1(i\omega_n), a_2(i\omega_n)) = 2 \left[(1+3a_1)(1+3a_2)t^4 + 2(1+2a_1+2a_2+3a_1a_2)t^2 + 2(1+a_1)(1+a_2) \right]$$

and

$$\mathcal{A}^{(2)}(\ell) = \frac{k_B T}{32} \sum_{n=0}^{\infty} \Delta_{1,\parallel} \Delta_{2,\parallel} p_n^4(\ell) \int_0^\infty t dt \frac{e^{-2p_n(\ell)\sqrt{t^2+1}}}{(t^2+1)} \tilde{g}^{(2)}(t, a_1(i\omega_n), a_2(i\omega_n), \theta) \quad (54)$$

with

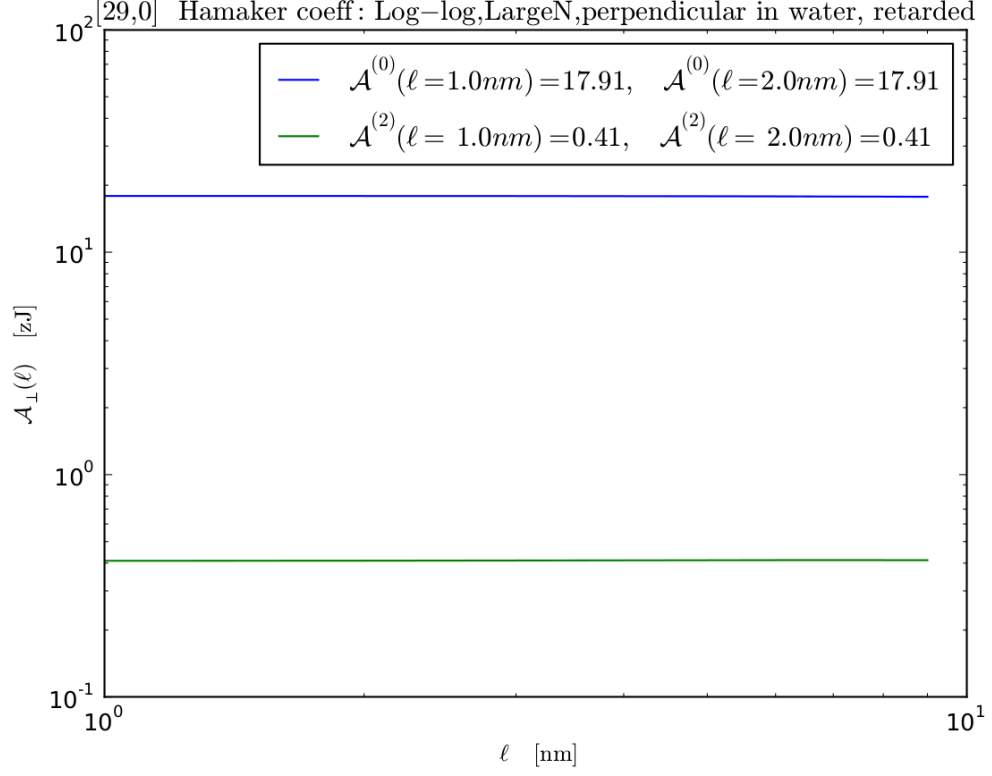


Figure 19: Full result

$$\tilde{g}^{(2)}(t, a_1(i\omega_n), a_2(i\omega_n), \theta) = (1 - a_1)(1 - a_2)(t^2 + 2)^2 \quad (55)$$

9.3 [29,0] Semi-log plot of $\mathcal{A}^{(0)}$ and $\mathcal{A}^{(2)}$

$$\mathcal{A}^{(0)}(\ell) = \frac{k_B T}{32} \sum_{n=0}^{\infty} \Delta_{1,\parallel} \Delta_{2,\parallel} p_n^4(\ell) \int_0^{\infty} t dt \frac{e^{-2p_n(\ell)\sqrt{t^2+1}}}{(t^2+1)} \tilde{g}^{(0)}(t, a_1(i\omega_n), a_2(i\omega_n)) \quad (56)$$

with

$$\begin{aligned} \tilde{g}^{(0)}(t, a_1(i\omega_n), a_2(i\omega_n)) = \\ 2 \left[(1 + 3a_1)(1 + 3a_2)t^4 + 2(1 + 2a_1 + 2a_2 + 3a_1a_2)t^2 + 2(1 + a_1)(1 + a_2) \right] \end{aligned}$$

and

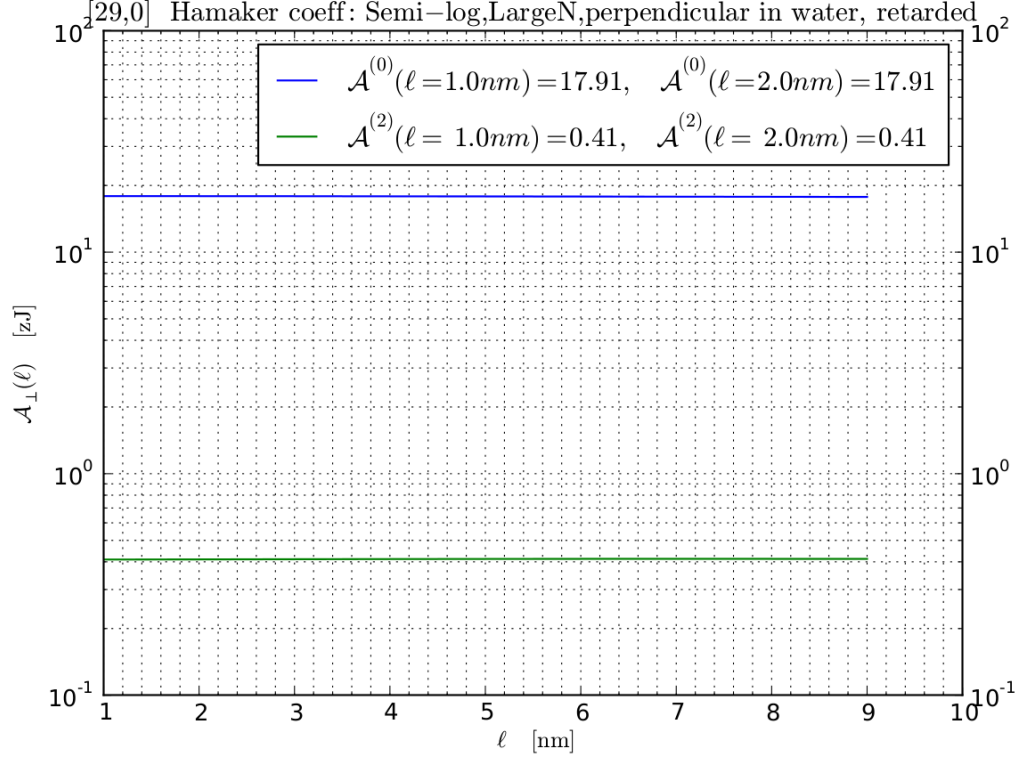


Figure 20: Full result

$$\mathcal{A}^{(2)}(\ell) = \frac{k_B T}{32} \sum_{n=0}^{\infty} \Delta_{1,\parallel} \Delta_{2,\parallel} p_n^4(\ell) \int_0^\infty t dt \frac{e^{-2p_n(\ell)\sqrt{t^2+1}}}{(t^2+1)} \tilde{g}^{(2)}(t, a_1(i\omega_n), a_2(i\omega_n), \theta) \quad (57)$$

with

$$\tilde{g}^{(2)}(t, a_1(i\omega_n), a_2(i\omega_n), \theta) = (1 - a_1)(1 - a_2)(t^2 + 2)^2 \quad (58)$$

Knee in plots of $\mathcal{A}^{(0)}$ as a function of separation

10 An example plot of knee: $\mathcal{A}^{(0)}$ for [9,3]

$$\mathcal{A}^{(0)}(\ell) = \frac{k_B T}{32} \sum_{n=0}^{\infty} \Delta_{1,\parallel} \Delta_{2,\parallel} p_n^4(\ell) \int_0^\infty t dt \frac{e^{-2p_n(\ell)\sqrt{t^2+1}}}{(t^2+1)} \tilde{g}^{(0)}(t, a_1(i\omega_n), a_2(i\omega_n)) \quad (59)$$

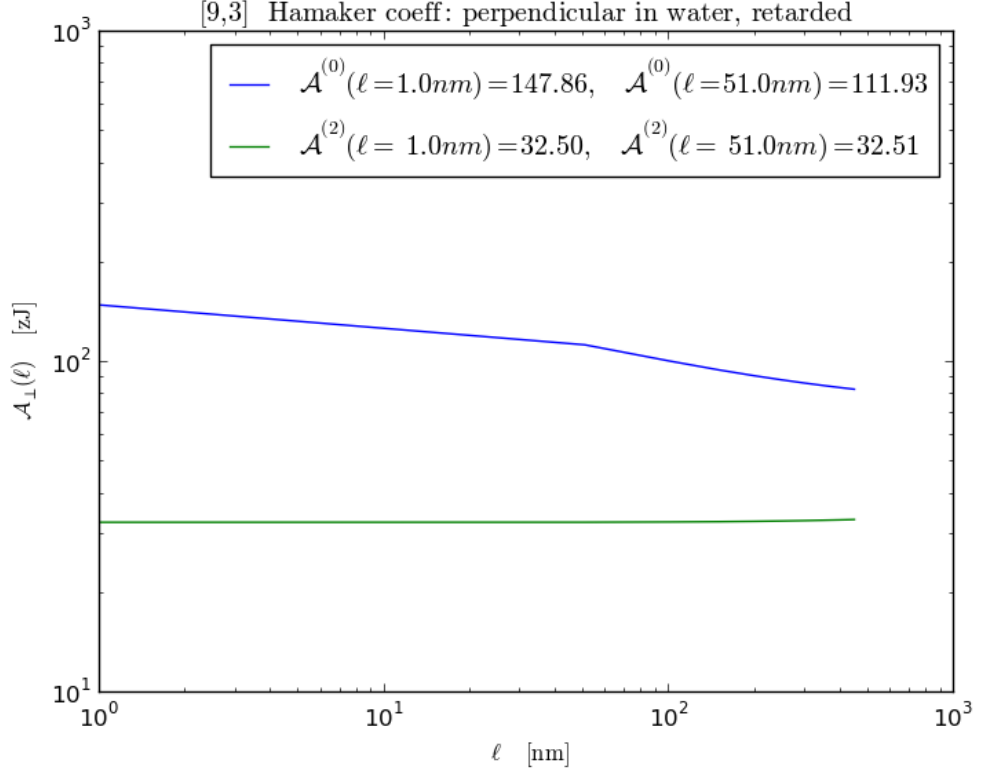


Figure 21: $\mathcal{A}^{(0)}$ as a function of separation appears to have a knee near 36 nm.

with

$$\begin{aligned} \tilde{g}^{(0)}(t, a_1(i\omega_n), a_2(i\omega_n)) = \\ 2 \left[(1 + 3a_1)(1 + 3a_2)t^4 + 2(1 + 2a_1 + 2a_2 + 3a_1a_2)t^2 + 2(1 + a_1)(1 + a_2) \right] \end{aligned}$$

and

$$\mathcal{A}^{(2)}(\ell) = \frac{k_B T}{32} \sum_{n=0}^{\infty} \Delta_{1,\parallel} \Delta_{2,\parallel} p_n^4(\ell) \int_0^\infty t dt \frac{e^{-2p_n(\ell)\sqrt{t^2+1}}}{(t^2+1)} \tilde{g}^{(2)}(t, a_1(i\omega_n), a_2(i\omega_n), \theta) \quad (60)$$

with

$$\tilde{g}^{(2)}(t, a_1(i\omega_n), a_2(i\omega_n), \theta) = (1 - a_1)(1 - a_2)(t^2 + 2)^2 \quad (61)$$

The (ℓ) dependence of the Hamaker coefficients \mathcal{A} is a consequence of (ℓ)

$$\text{dependence of } p_n^2(\ell) = \epsilon_m(i\omega_n) \frac{\omega_n^2}{c^2} \ell^2$$

$$\mathcal{A}^{(0)}(\ell) = \frac{k_B T}{32} \sum_{n=0}^{\infty} \Delta_{1,\parallel} \Delta_{2,\parallel} p_n^4(\ell) \int_0^\infty t dt \frac{e^{-2p_n(\ell)\sqrt{t^2+1}}}{(t^2+1)} \tilde{g}^{(0)}(t, a_1(i\omega_n), a_2(i\omega_n)) \quad (62)$$

with

$$\tilde{g}^{(0)}(t, a_1(i\omega_n), a_2(i\omega_n)) = 2 \left[(1+3a_1)(1+3a_2)t^4 + 2(1+2a_1+2a_2+3a_1a_2)t^2 + 2(1+a_1)(1+a_2) \right] \quad (63)$$

and

$$\mathcal{A}^{(2)}(\ell) = \frac{k_B T}{32} \sum_{n=0}^{\infty} \Delta_{1,\parallel} \Delta_{2,\parallel} p_n^4(\ell) \int_0^\infty t dt \frac{e^{-2p_n(\ell)\sqrt{t^2+1}}}{(t^2+1)} \tilde{g}^{(2)}(t, a_1(i\omega_n), a_2(i\omega_n), \theta) \quad (64)$$

with

$$\tilde{g}^{(2)}(t, a_1(i\omega_n), a_2(i\omega_n), \theta) = (1-a_1)(1-a_2)(t^2+2)^2 \quad (65)$$

$\zeta_n = 2\pi n k_B T / \hbar$, where n is an integer and the $n = 0$ term is counted with a weight $1/2$.

where $p_n^2(\ell) = \epsilon_m(i\omega_n) \frac{\omega_n^2}{c^2} \ell^2$.

11 Plots of how each Matsubara term contributes to $\mathcal{A}_n^{(0)}(\ell)$

11.1 Plots for visualizing and comparing gradients for different CNT's

Surface plots for Hamaker Coefficients as function of angle and separation

12 Fully Retarded

12.1 $\mathcal{A}^{(0)}$ for [6,5], [9,1], and [29,0] in water

$$\mathcal{A}^{(0)}(\ell) = \frac{k_B T}{32} \sum_{n=0}^{\infty} \Delta_{1,\parallel} \Delta_{2,\parallel} p_n^4(\ell) \int_0^\infty t dt \frac{e^{-2p_n(\ell)\sqrt{t^2+1}}}{(t^2+1)} \tilde{g}^{(0)}(t, a_1(i\omega_n), a_2(i\omega_n)) \quad (66)$$

with

$$\tilde{g}^{(0)}(t, a_1(i\omega_n), a_2(i\omega_n)) = 2 \left[(1+3a_1)(1+3a_2)t^4 + 2(1+2a_1+2a_2+3a_1a_2)t^2 + 2(1+a_1)(1+a_2) \right] \quad (67)$$

and

[6,5] Gradient $\mathcal{A}^{(0)}$ terms : perpendicular in water, retarded

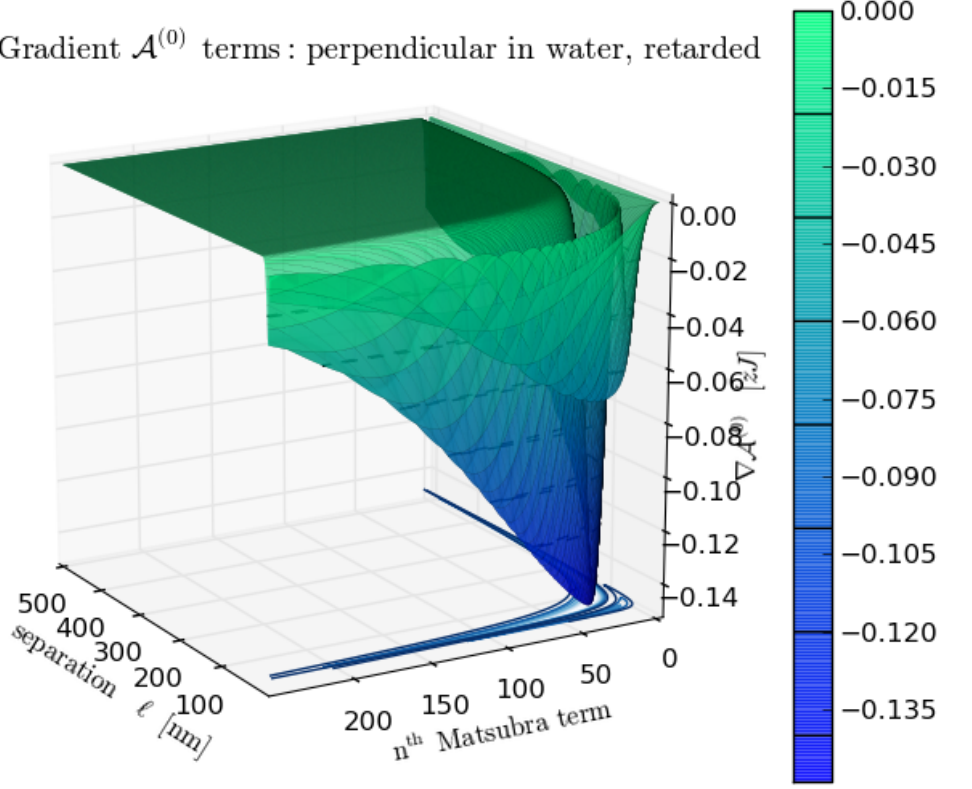


Figure 22: $\nabla(\mathcal{A}_n^{(0)}(\ell))$ for [6,5]: derivative of $\mathcal{A}_n^{(0)}(\ell)$ (z-axis) with respect to separation and n (x and y axes. $Max[|\nabla(\mathcal{A}^{(0)})|]$ occurs at $\ell = \ell_{knee}$

$$\mathcal{A}^{(2)}(\ell) = \frac{k_B T}{32} \sum_{n=0}^{\infty} \Delta_{1,\parallel} \Delta_{2,\parallel} p_n^4(\ell) \int_0^\infty t dt \frac{e^{-2p_n(\ell)\sqrt{t^2+1}}}{(t^2+1)} \tilde{g}^{(2)}(t, a_1(i\omega_n), a_2(i\omega_n), \theta) \quad (68)$$

with

$$\tilde{g}^{(2)}(t, a_1(i\omega_n), a_2(i\omega_n), \theta) = (1 - a_1)(1 - a_2)(t^2 + 2)^2 \quad (69)$$

[9,1] Gradient $\mathcal{A}^{(0)}$ terms : perpendicular in water, retarded

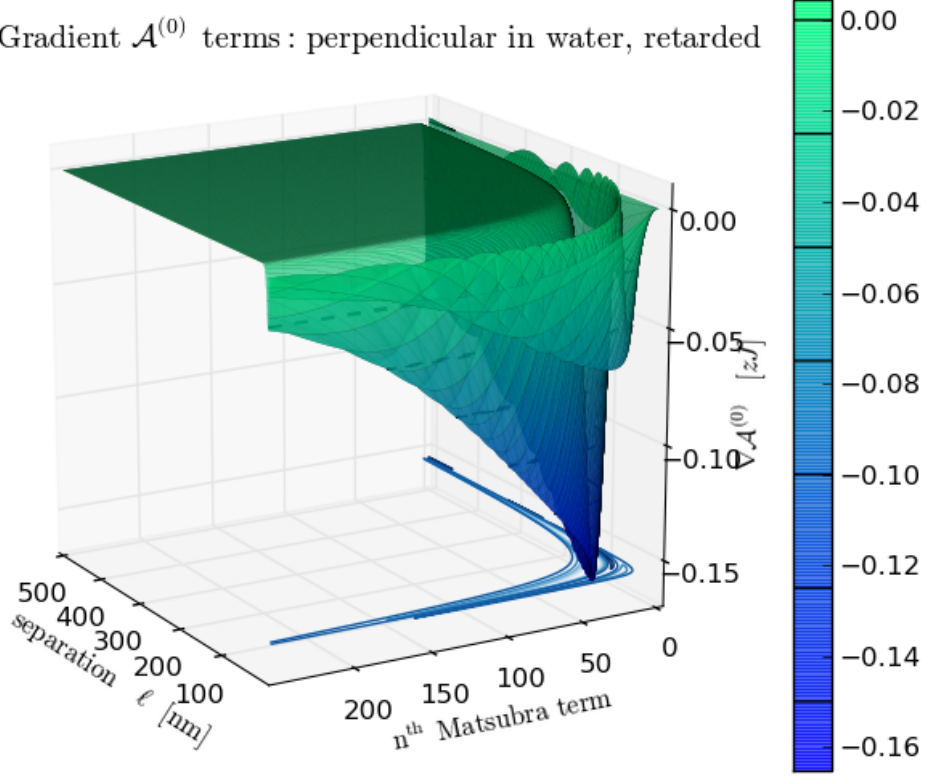


Figure 23: $\nabla(\mathcal{A}_n^{(0)}(\ell))$ for [9,1]: derivative of $\mathcal{A}_n^{(0)}(\ell)$ (z-axis) with respect to separation and n (x and y axes. $Max[|\nabla(\mathcal{A}^{(0)})|]$ occurs at $\ell = \ell_{knee}$

12.2 Hamaker 2: $\mathcal{A}^{(2)}$ for [6,5], [9,1], and [29,0] in water

$$\mathcal{A}^{(0)}(\ell) = \frac{k_B T}{32} \sum_{n=0}^{\infty} \Delta_{1,\parallel} \Delta_{2,\parallel} p_n^4(\ell) \int_0^\infty t dt \frac{e^{-2p_n(\ell)\sqrt{t^2+1}}}{(t^2+1)} \tilde{g}^{(0)}(t, a_1(i\omega_n), a_2(i\omega_n)) \quad (70)$$

with

$$\tilde{g}^{(0)}(t, a_1(i\omega_n), a_2(i\omega_n)) = 2 [(1+3a_1)(1+3a_2)t^4 + 2(1+2a_1+2a_2+3a_1a_2)t^2 + 2(1+a_1)(1+a_2)] \quad (71)$$

and

[9,3] Gradient $\mathcal{A}^{(0)}$ terms : perpendicular in water, retarded

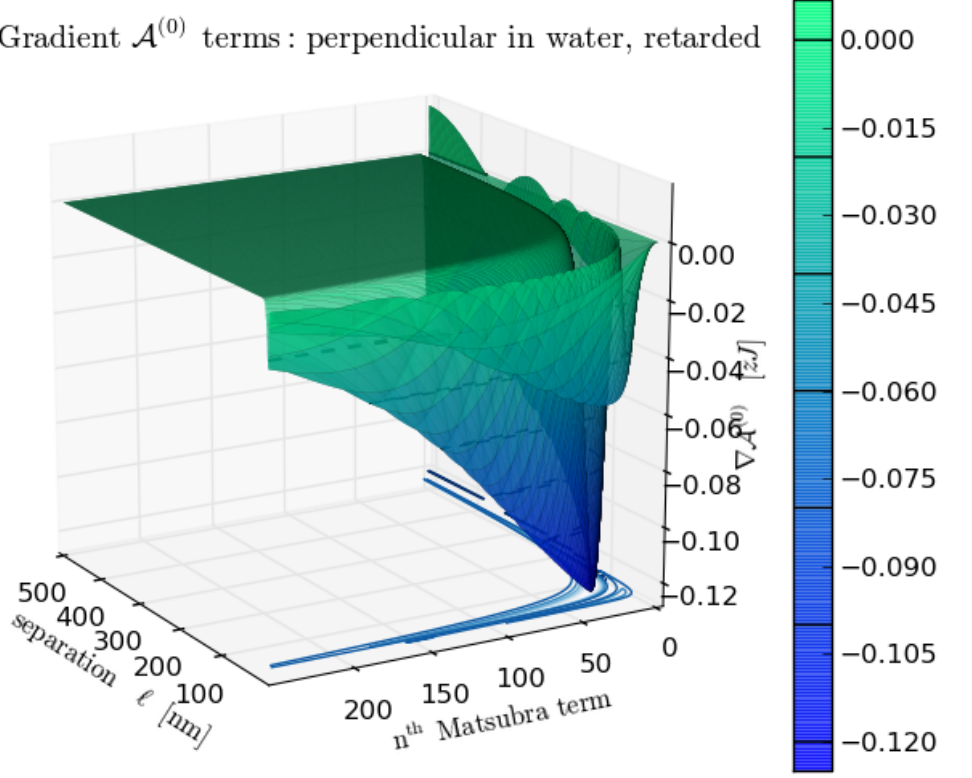


Figure 24: $\nabla(\mathcal{A}_n^{(0)}(\ell))$ for [9,3]: derivative of $\mathcal{A}_n^{(0)}(\ell)$ (z-axis) with respect to separation and n (x and y axes. $Max[|\nabla(\mathcal{A}^{(0)})|]$ occurs at $\ell = \ell_{knee}$

$$\mathcal{A}^{(2)}(\ell) = \frac{k_B T}{32} \sum_{n=0}^{\infty} \Delta_{1,\parallel} \Delta_{2,\parallel} p_n^4(\ell) \int_0^\infty t dt \frac{e^{-2p_n(\ell)\sqrt{t^2+1}}}{(t^2+1)} \tilde{g}^{(2)}(t, a_1(i\omega_n), a_2(i\omega_n), \theta) \quad (72)$$

with

$$\tilde{g}^{(2)}(t, a_1(i\omega_n), a_2(i\omega_n), \theta) = (1 - a_1)(1 - a_2)(t^2 + 2)^2 \quad (73)$$

[29,0] Gradient $\mathcal{A}^{(0)}$ terms : perpendicular in water, retarded

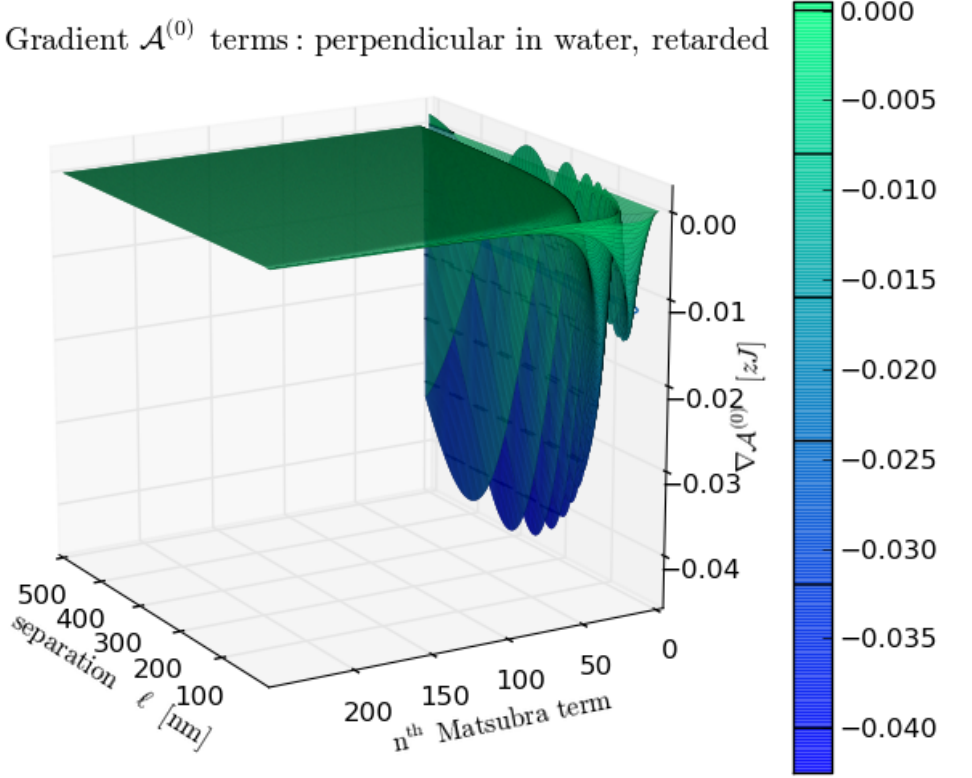


Figure 25: $\nabla(\mathcal{A}_n^{(0)}(\ell))$ for [29,0]: derivative of $\mathcal{A}_n^{(0)}(\ell)$ (z-axis) with respect to separation and n (x and y axes. $Max[|\nabla(\mathcal{A}^{(0)})|]$ occurs at $\ell = \ell_{knee}$

12.3 Total Hamaker: $\mathcal{A} = \mathcal{A}^{(0)} + \mathcal{A}^{(2)}$ for [6,5], [9,1], and [29,0] in water

$$\mathcal{A}^{(0)}(\ell) = \frac{k_B T}{32} \sum_{n=0}^{\infty} \Delta_{1,\parallel} \Delta_{2,\parallel} p_n^4(\ell) \int_0^\infty t dt \frac{e^{-2p_n(\ell)\sqrt{t^2+1}}}{(t^2+1)} \tilde{g}^{(0)}(t, a_1(i\omega_n), a_2(i\omega_n)) \quad (74)$$

with

$$\tilde{g}^{(0)}(t, a_1(i\omega_n), a_2(i\omega_n)) = 2 \left[(1+3a_1)(1+3a_2)t^4 + 2(1+2a_1+2a_2+3a_1a_2)t^2 + 2(1+a_1)(1+a_2) \right] \quad (75)$$

and

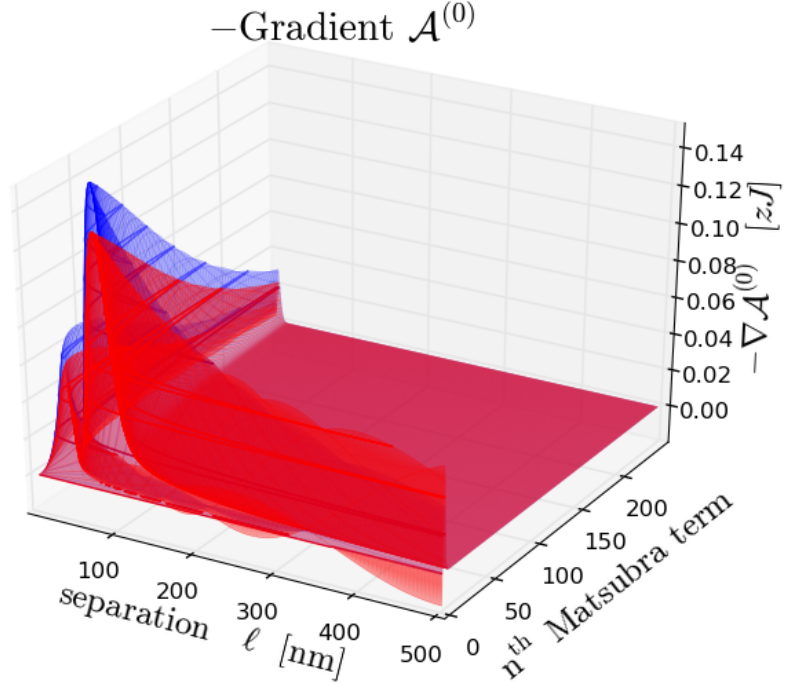


Figure 26: $-\nabla(\mathcal{A}_n^{(0)}(\ell))$ for [6,5] (blue) and [9,3] (red)

$$\mathcal{A}^{(2)}(\ell) = \frac{k_B T}{32} \sum_{n=0}^{\infty} \Delta_{1,\parallel} \Delta_{2,\parallel} p_n^4(\ell) \int_0^\infty t dt \frac{e^{-2p_n(\ell)\sqrt{t^2+1}}}{(t^2+1)} \tilde{g}^{(2)}(t, a_1(i\omega_n), a_2(i\omega_n), \theta) \quad (76)$$

with

$$\tilde{g}^{(2)}(t, a_1(i\omega_n), a_2(i\omega_n), \theta) = (1 - a_1)(1 - a_2)(t^2 + 2)^2 \quad (77)$$

Tables

13 Table of published results

14 Table of python results

*data from Chirality-dependent properties of carbon nanotubes: electronic structure, optical dispersion properties, Hamaker coefficients and van der

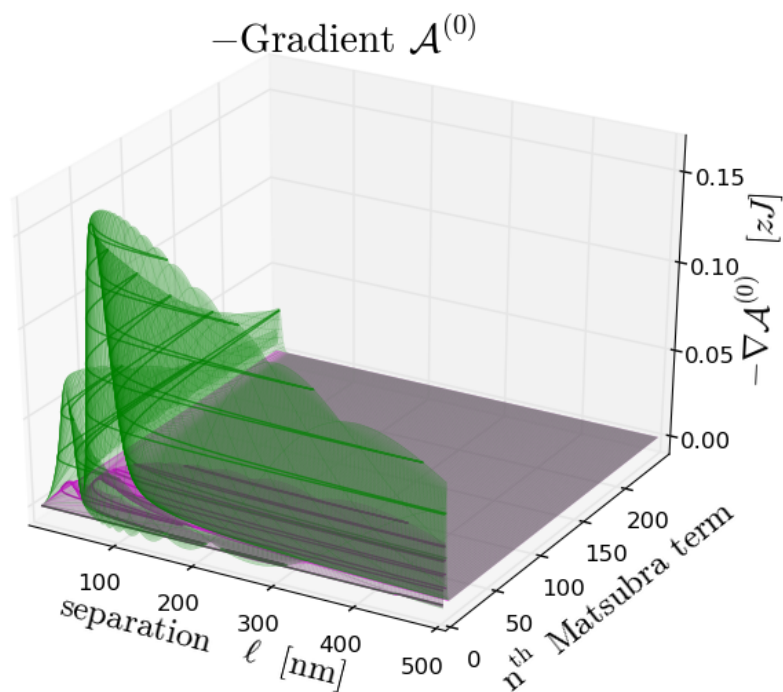


Figure 27: $-\nabla(\mathcal{A}_n^{(0)}(\ell))$ for [9,1] (green) and [29,0] (magenta)

WaalsLondon dispersion interactions Rick F. Rajter, Roger H. French, W.Y. Ching, Rudolf Podgornik and V. Adrian Parsegian RSC Adv., 2013,3, 823-842
DOI: 10.1039/C2RA20083J

15 Table of Gecko Hamaker results

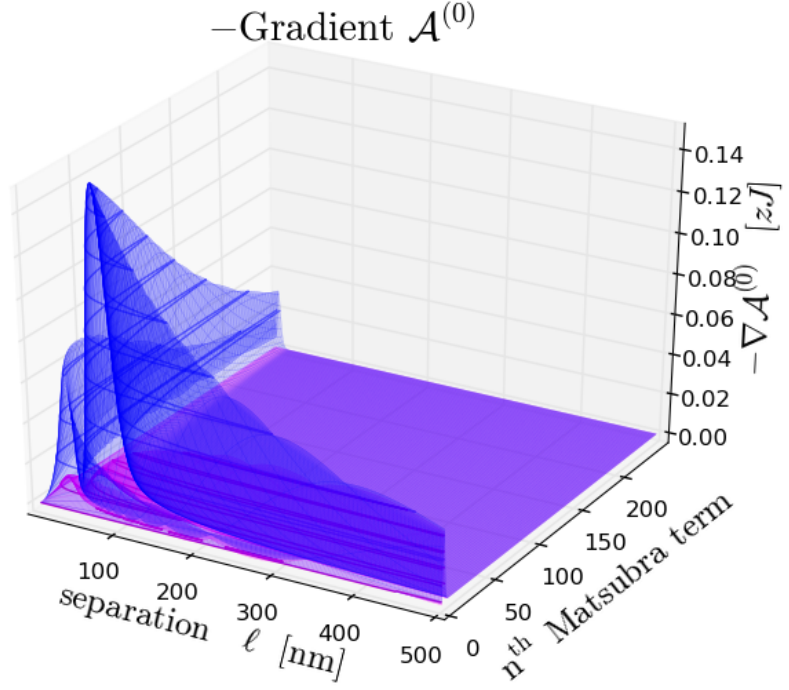


Figure 28: $-\nabla(\mathcal{A}_n^{(0)}(\ell))$ for [6,5] (blue) and [29,0] (magenta)

Table 1: Rajter results from IJMR perpendiucalar cylinders in water (Rajter's spectrum)

CNT	\mathcal{A}^0 [zJ]	\mathcal{A}^2 [zJ]
[6,5]	106	1.9
[9,0]	-	
[9,1]	92.8	3
[9,3]	107	36.2
[29,0]	18.5	0.8

Table 2: Python results, retarded formulation: perpendiucalar cylinders in water, intersurface distance = 1 nm

CNT	atoms*	radius*[A]	Type*	Geom*	$\mathcal{A}^0(n=0)$ [zJ]	\mathcal{A}^0 [zJ]	\mathcal{A}^2 [zJ]
[6,5]	364	3.734	sc	chiral	1x5.46	105.46	0.96
[9,0]			semi-metal; in progress				
[9,1]	364	3.734	sc	chiral	1x5.46	93.56	1.56
[9,3]	156	4.234	sm	chiral	1x5.46	83.06	3.23
[29,0]	116	11.352	sc	zigzag	1x5.46	17.73	0.41

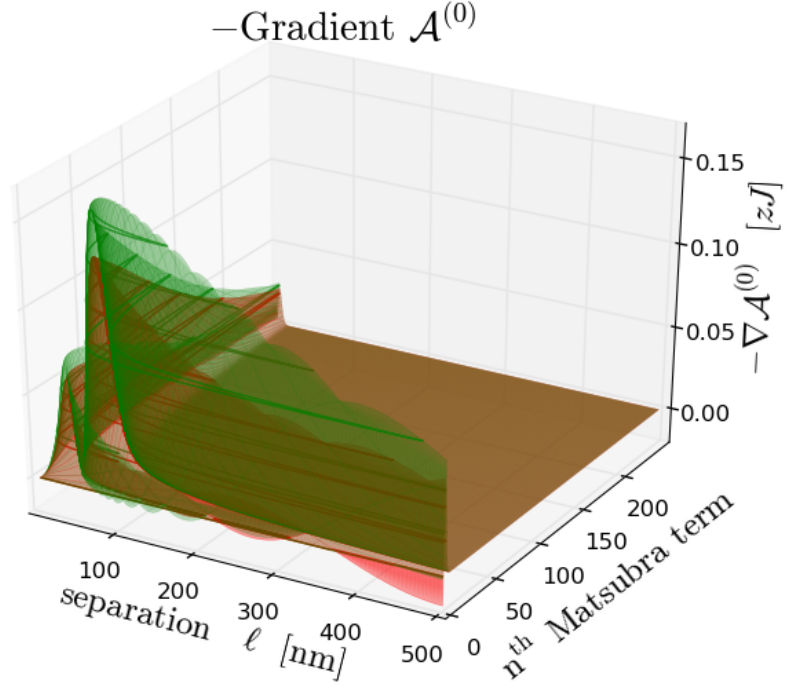


Figure 29: $-\nabla(\mathcal{A}_n^{(0)}(\ell))$ for [9,1] (red) and [9,3] (green)

Table 3: Python results, non-retarded formulation: perpendiucalar cylinders in water

CNT	\mathcal{A}^0 [zJ]	\mathcal{A}^2 [zJ]
[6,5]	126.80	1.16
[9,0]	semi-metal; in progress	
[9,1]	112.22	1.87
[9,3]	semi-metal; in progress	
[29,0]	20.93	0.49

Table 4: Gecko Hamaker results from 2.07, perpendiucalar cylinders in water

CNT	\mathcal{A}^0 [zJ]	\mathcal{A}^2 [zJ]
[6,5]	100	1.04
[9,0]	151	6.96
[9,1]	84.85	1.16
[9,3]	80.66	1.55
[29,0]	17.68	0.22

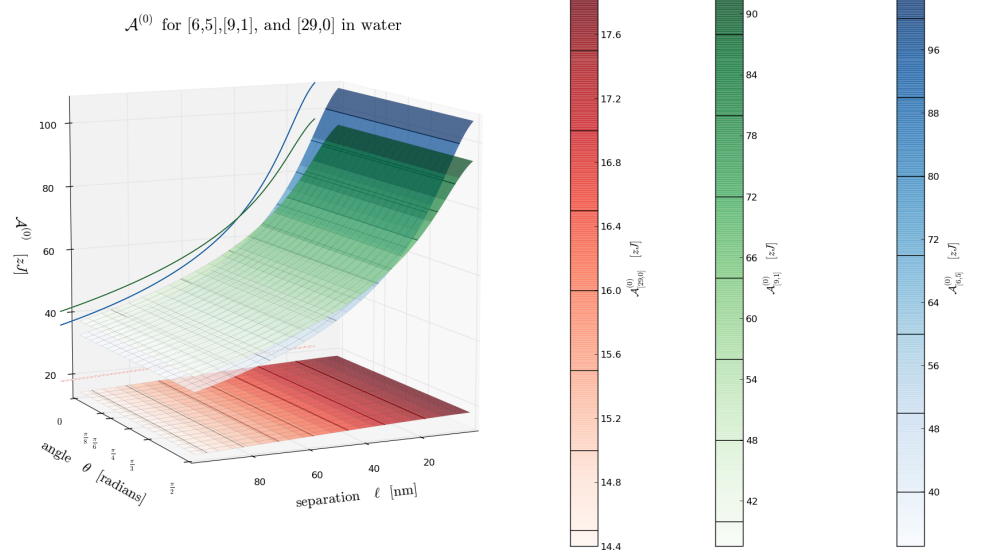


Figure 30: $\mathcal{A}^{(0)}$ for [6,5], [9,1], and [29,0] in water. No theta dependence

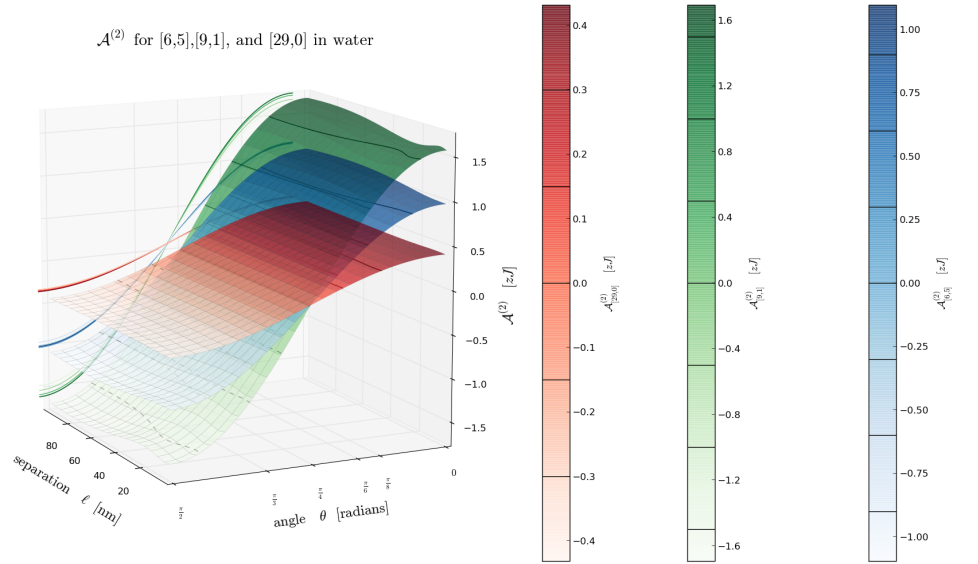


Figure 31: $\mathcal{A}^{(2)}$ for [6,5], [9,1], and [29,0] in water.

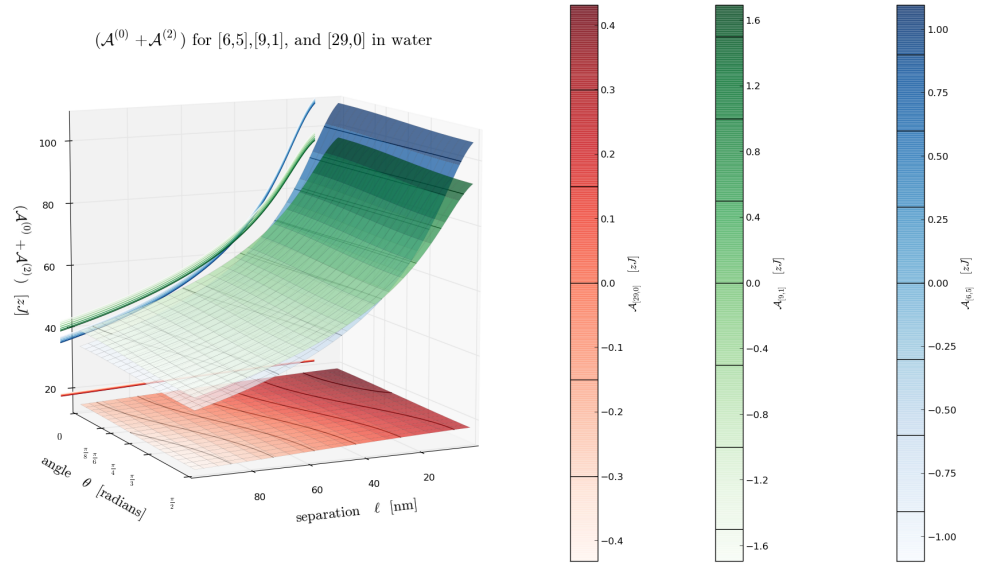


Figure 32: $\mathcal{A} = \mathcal{A}^{(0)} + \mathcal{A}^{(2)}$ for [6,5], [9,1], and [29,0] in water